Automatic 3D modelling of train rails in a lidar point cloud

DANIEL DÍAZ BENITO
February 2012

SUPERVISORS:

Dr. K. Khoshelham
Dr. Ir. S.J. Oude Elberink

Automatic 3D modeling of train rails in a lidar point cloud

DANIEL DÍAZ BENITO

Enschede, The Netherlands, February, 2012

ABSTRACT

Rail track irregularities have a large effect on railway safety and operation. To ensure a good maintenance of the rails, frequent measurements are needed, which are costly and require specific tools for different aspects of the rails geometry. Laser scanning offers the advantage of acquiring accurate 3D measurements of all the objects present in the railway environment in a short operational time. While some work has been done to detect the presence of rails and other objects in the point cloud, the modelling of those objects has received little attention. Such models not only enable all sorts of measurements about the rail geometry, but also facilitate simulations in train research. The purpose of this thesis is to develop a method to automatically build a 3D model of train rails from a point cloud where the rails have been already detected. First of all, the rail point cloud is sectioned into pieces of equal length. The points laying in each of the planes of the head of the rail are then identified. A non-linear least squares adjustment is used to find the parameters of the model pieces that best fit into the point cloud by minimizing the distance from the points to their corresponding planes. Finally, the model pieces are adjusted globally using a 6 dimensional non-rational Bezier curve, which yields a set of rail profiles that can be connected to build the final model representing the curved shape of the rail. The final model is validated by computing the distance from each point in the point cloud to the end model. The results showed that 90% of the points were at less than 1 cm distance to the reconstructed model, while the mean distance is 0.5 cm and 95% of the points were at less than 1.4 cm. Although the results are dependent on the accuracy of acquisition and detection methods, the overall performance of the method demonstrates that it is possible to model the train rails accurately by surface fitting and curvature adjustment.

ACKNOWLEDGEMENTS

TABLE OF CONTENTS

LIST OF FIGURES

LIST OF TABLES

1. INTRODUCTION

1.1. Motivation

With the spread of high-speed trains and the increasing costs of road transport, railway research for technical improvements and cost reduction has increased notably during the last decade. One of the main focuses has been on the rail track. Rail track irregularities have a large effect on different aspects of railway operation, mainly system safety, train speed optimization, movement behaviour and passenger comfort. Indeed, according to the Federal Railroad Administration Office of Safety Analysis (2011), 16% of the railway accidents in the US from 1975 to 2011 have been caused by an incorrect geometry of the tracks due to deformations.

Consequently, railway infrastructure companies invest yearly large amounts of money in rail track maintenance. A key point in this activity is regular inspection of the rail status in order to avoid performance problems or unsafe situations. The critical factors of this inspection are speed and accuracy of the rails geometry measurement system.

Actual developments in rail track inspection methods have been reviewed by Papaelias et al. (2008). These methods are divided into contact and non-contact measurements. The major problems with contact techniques are that they produce rail wear and due to speed requirements, they limit the operability of the train corridor. On the other hand, the non-contact methods include accelerometer and gyroscope devices which are affected by the train vibrations and cannot assess the wear of the rail surface (Grassie, 1996; Weston et al., 2007). Therefore optical methods seem to have advantages and have been used for accurate measurements of the rails profile (Alippi et al., 2002).

But the importance of acquiring accurate geometry of the rails is not limited to railway inspection, and also involves providing information for further research on deterioration modelling. Sadeghi & Askarinejad (2010) and Guler et al. (2011) show the opportunities for maintenance and economical planning in rail deterioration modelling, and systematical acquisition of the rails geometry can improve the development of those models. Additionally, accurate track reconstruction data is a basic requisite on simulation research to improve vehicle design testing and performance optimization (Evans & Berg, 2009; Li, Meddah, Hass, & Kalay, 2006).

In order to obtain this data, railway companies often use manual inventories, hand devices or the aforementioned contact tools. The manual techniques are dependant of the operator criteria, and the required long interruptions of the track operation results costly. Whereas for the contact tools, it requires different and specific machines for every parameter to be measured, increasing the maintenance costs.

In contrast, mobile laser scanning seems to be suitable in order to gather all the required data at a time, independent of lighting limitations, and providing better measurement accuracy. The problem is that a methodology to classify and model the rail track from laser data did not exist up to now.

1.2. Literature review

Although computer vision techniques have been applied to extract some objects of the railway scene (Marino, Distante, Mazzeo, & Stella, 2007; Mazzeo, 2004), those researches have focused on recognizing the bolts in the rails, and they face clear limitations to generate accurate measurements of rails and other objects.

On the other hand, recent work by Neubert et al. (2008) has explored the possibility of extracting the rail track from helicopter-borne lidar point clouds using RANSAC and profile knowledge classification. In combination with high resolution aerial imagery, Beger, Gedrange, Hecht and Neubert (2011), have used also laser scanning data to retrieve the main axis of railway tracks.

Nevertheless, those techniques focus in detecting the points of the object, but the relationship between the points have been not reconstructed, thus limiting the type of measurements that can be done and being not suitable as visualization for some applications. On the other hand, modelling of certain objects using laser scanning point clouds has been addressed for surfaces as roads (Jaakkola, Hyyppa, Hyyppa, & Kukko, 2008), linear objects as power lines (Jwa & Sohn, 2010) and complex objects as industrial installations (Rabbani, 2006), but not for complex linear objects as rails.

1.3.   Objectives and research questions

1.3.1.   Research objectives

The general goal of the research is to develop a method to automatically generate a 3D vector representation of the rails from a point cloud of the railway environment. As classification of this type of point cloud has been the topic of another research at ITC (Arastounia, 2012), this project focuses on geometric modelling of the rails and their tracks. Therefore, the methodology developed here directly applies to an already classified laser scanning point cloud, where some points have been already detected as feasible candidates to be part of the rail.

The produced model is intended to be valid for geometrical measurements. Although the final use of the model is stressed over maintenance and inventory issues, it is open enough to act as relevant input data for vehicle designers or train driving simulators.

1.3.2.   Research questions

- Can laser range data be effectively used to extract 3D vector models of train rails?

- What are the requirements of the data in order to make possible the modelling?

- What is the internal accuracy of the gauge measurement from the reconstructed rail model?

- Is it possible to detect misclassified points during the modelling process?

- How the different faces of the rail geometry can be identified in the point cloud?

- What algorithm can be used to model the curvature of rail objects?

- What are the parameters that allow fitting the primitives that compose a rail model?

1.4.   Outline of thesis

The rest of the thesis is organised as follows: In Chapter 2, background information about the rail object, the different types present in nowadays railways, the dataset used as input for the study and the characteristics of the acquisition method are presented.

Next, in Chapter 3, the methods to accomplish the task are described, from the model characteristics to the final output format, including the fitting methods and statistical analysis used in the final validation of the resulting model.

The results of the study as applied to the available dataset are presented in Chapter 4, including a discussion about their traits, characteristics of the specific problem that arose with the analysis, as well as consequences of certain variables decisions and limitations of the method.

A final summary is outlined in Chapter 5, including a list of strengths and weaknesses of the methodology, in addition to possible follow-ups than can improve it, and different approaches that can face new challenges and opportunities regarding this modelling problem.

2.   BACKGROUND

2.1.   Existing rail designs in the Netherlands

There are three main rail types in use in the Netherlands:

* NP 46: an old rail design used in wooden sleepers tracks.

* UIC 54: the standard rail design used in all the new projects.

* UIC 60 (E1): used for freight and high-speed tracks.

Detailed information about the measurements of these rails has been provided by Movares. Although UIC 60 is of common use throughout Europe, the model used in this research has been based on the UIC 54 as it is the only rail model present in the available dataset.

The basic traits of this steel rail are 70 mm width in the top, 159 mm of total height, 140 mm width in the base and 16 mm width in the body.
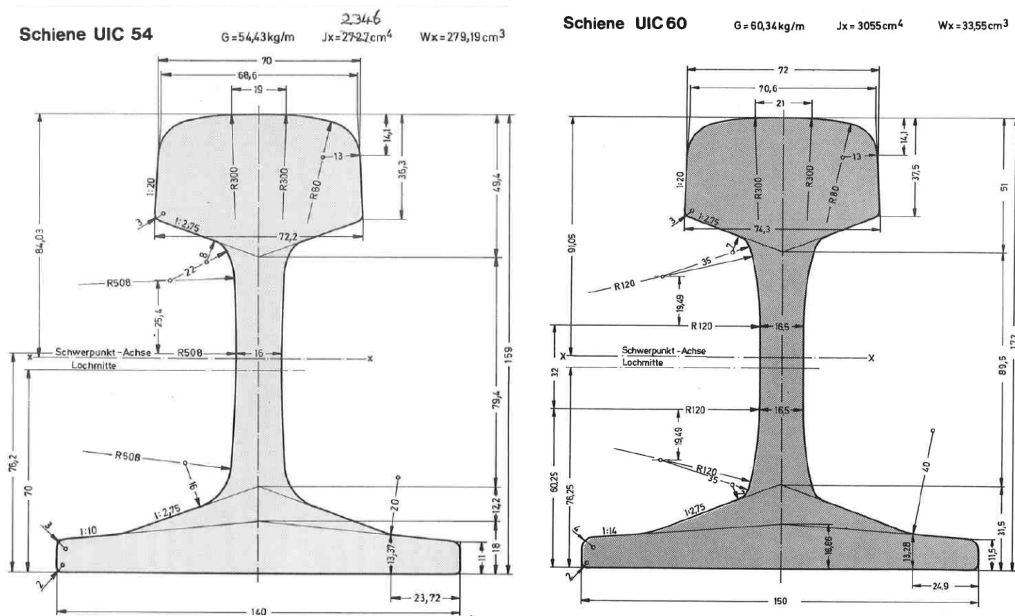
Figure 1: Design parameters of an UIC 54 rail profile. Source: Movares.

Throughout this document the rail will be divided in 3 parts with the name of head, web and foot, describing the top part, the linking central part and the base of the rail respectively.

2.2.   Actual measurements techniques

Besides the visual inspections run by the railway maintenance crew, there are two main types of rail measurements: internal rail inspections and track geometry measurements. Internal rail inspection provides information about the rail or track structure and is traditionally assessed using ultrasonic techniques, or ground penetrating radar in the case of the track bed.

Whereas for the geometry measurements are obtained manually using hand tools or electronic devices, but in the past decades the uses of track geometry cars that can do the measurements automatically have widespread. In addition to the higher rate of measurement, they have also the advantage of measuring the rail 'in load' as they represent a considerable weight over the track. They are based typically on contact or optical techniques able to measure the vertical and lateral deviations, but also systems based in accelerometers have been tested to check these deviations.

Finally, high resolution images have been applied also to crack detection in the rail or other elements of the track, although these techniques still require human visual review.

2.3. Overview of data acquisition and preprocessing of point clouds

Although point clouds can be obtained by processing a series of registered images, they are more commonly obtained from laser scanning. These systems can be divided in three main categories depending on the way the laser device moves along the observed surface: terrestrial, airborne and mobile.

In terrestrial laser scanning, the laser device is placed at one location and the environment is scanned from that spot obtaining a point cloud of the scene. These systems have often higher accuracy but are time consuming because of the registration process of the different point clouds and the relocation of the device to record large objects.

In contrast, airborne laser scanner sends the laser device to the sky to scan the surface of the Earth along planned strips. It requires complex navigation systems able to register the point cloud taking into account the movements of the aircraft, but it can efficiently register large surfaces and is thus often used to obtain topographic features. Still, the improvements in these systems have allowed going down and analyze smaller objects, as houses, trees or street objects. Nevertheless, shipping a full equipped aircraft can be a costly mission that requires reusing the data to make it economically viable, and after all, the level of detail and the vertical point of view can be not suitable for some applications.

Finally, in mobile laser scanning a car is used to move the device while acquiring the surrounding scene. In the case of railways, this is often done by modifying the car so it can run over the track. The system requires navigation equipment similarly as for the airborne case, although the point density is higher due to the proximity to the observed object. This scanning typology frequently is limited by the lateral occlusion of objects in the surrounding, although the use of multiple strips can alleviate this. Even so, because of the more affordable costs in comparison with airborne laser scanning, and the safety position while acquiring data in highways, streets and railways, it has been used in the last years for an increasing number of applications.

Processing of point clouds often involves different phases where different strips are registered and combined, often after a noise reduction level step. Depending on the application, some objects may be detected and reconstructed using model or data driven approaches. While the first one try to fit some kind of geometry to the point cloud, data driven fits planes to the data and tries to reconstruct the object from them.

Another common operation when handling point clouds is segmentation. This step tries to group the points following a set of properties, as distribution or proximity, labelling them to further process the points.

A detailed overview of these acquisition methods can be found at Vosselman & Maas (2010).

2.4.   Description of data used in this research

2.4.1.   Original data

The original dataset used for the whole project was kindly provided by the Movares company. It consisted in a 700 m long point cloud located near the city of Elst in The Netherlands. It includes one station platform, one crossroad junction, towers, wires, trees and two tracks separated by a linear mound, and consisting in a total of four straight rails (see Figure 2).
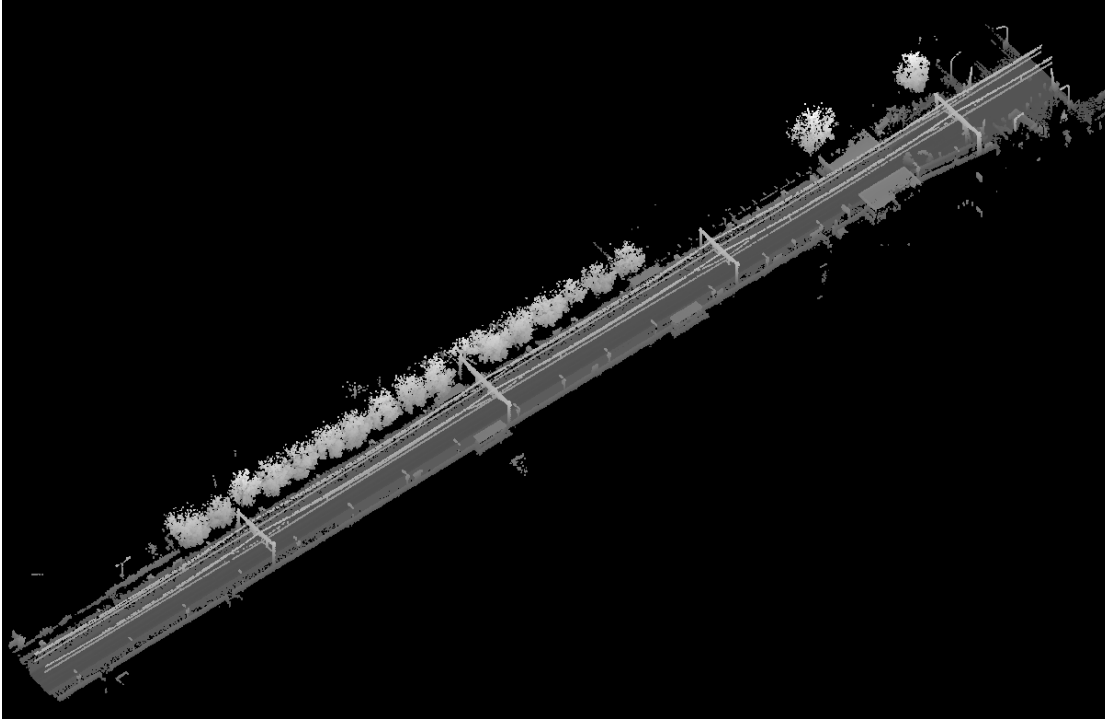
Figure 2: Fragment of the original point cloud dataset. Source: Movares.

The dataset was acquired by a mobile laser scanning device mounted over a modified van running over the rail track. The point cloud was produced by registering more than one strip, although the exact details about the procedure and the laser device are unknown. The dataset as provided seems also to have passed through an atmospheric noise cleaning.

2.4.2.   Input data

The input data for this research was the detected rail points as produced by Arastounia (2012). This dataset is a 90 m long subset of the original, and it was chosen in the other study to reduce the processing time of the experiments, while being still representative of the entire dataset, having crossroad junctions, towers, wires and straight rails.

Two different datasets were provided by that study, one using region growing and another using template matching, both obtained from the same original dataset. Unless expressed otherwise, it must be assumed the results presented in this document correspond to those obtained using the region growing dataset as input.

Throughout this document the four rails contained in the dataset have been numbered following a West-East criterion, so the western rail is identified as rail 1 and the eastern one as rail 4. The input dataset already includes a label for each point telling to what rail, and even what track pair, they belong, so the points of the individual rails are automatically identifiable as can be appreciated in Figure 3.
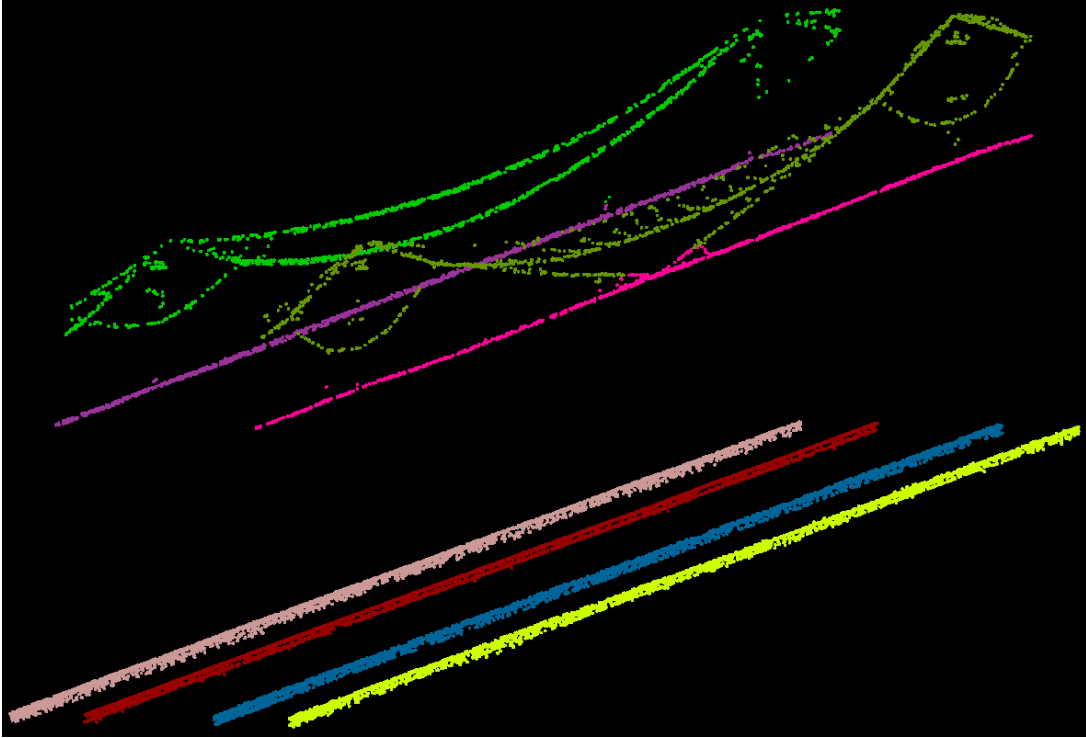
Figure 3: Input dataset. Rails are identified in the bottom by colour from 1 (left of the image) to 4 (right).

The input dataset preserved the mm precision of the original data.

3. PARAMETRIC MODELLING OF RAILS IN POINT CLOUD DATA

3.1. Overview of the methodology

This thesis proposes a methodology composed by three different phases and a total of eight steps as outlined in Figure 4. In the first phase, the point cloud is prepared to fit the model, starting by sectioning it in thin rail pieces so it can be assumed that the rail is approximately straight in the given section. Then points with extreme values are detected and removed from the next steps to decrease the number of wrong results. As the fitting phase requires values for the starting parameters, an initial estimation is done for them using basic stats of the point cloud. In addition, the fitting algorithm requires the implicit function of the plane where each point lies, and so, this relationship has to be identified labelling each point with the id of its correspondent plane.
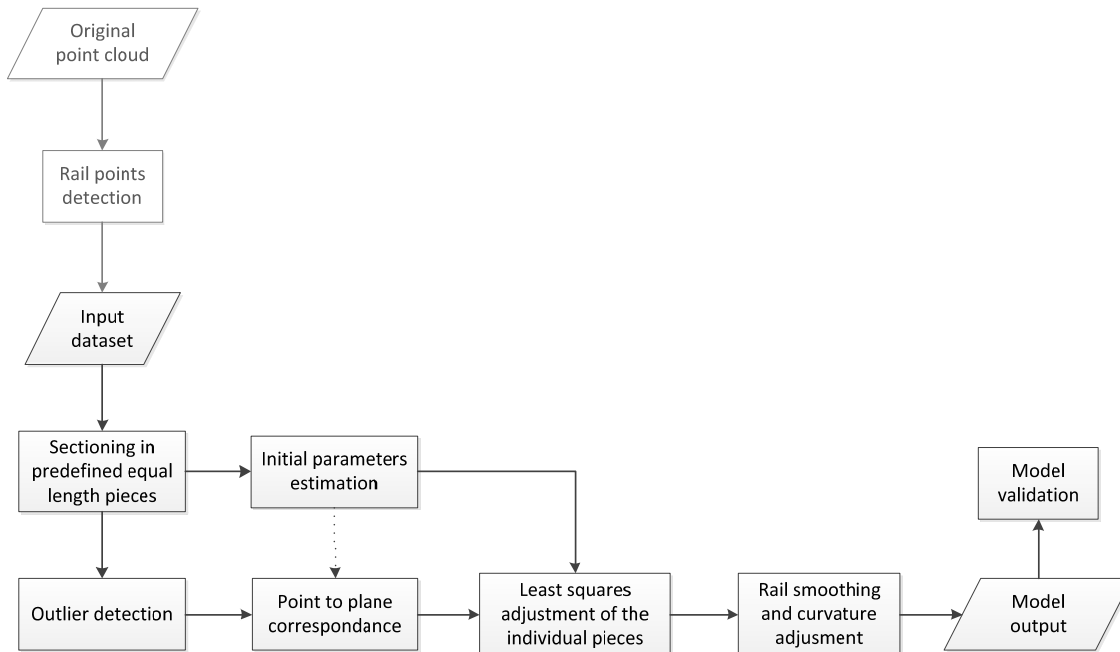
Figure 4: Diagram of the thesis methodology processing phases.

In the case of the fitting phase two different approaches have been tested using 2D and 3D models. The 2D method was designed to model not only the location of the rail but also the wear suffered by train usage and to estimate the shape of the rail when it is not known. Because of some limitations on projecting the point cloud to a 2D rail profile the 3D approach was developed. However, in that 3D approach only the translation and rotation of the rail are reconstructed, assuming the rail type is known and the wear is not relevant in comparison with the point cloud accuracy. These two assumptions are necessary to make the process automatic, avoiding the manual steps used in the 2D approach.

During the fitting phase a least squares adjustment is used to minimize the algebraic distance of each observation to its corresponding plane, understanding as observation every point in the dataset. This is

done by adjusting the unknown parameters of the model, which are the translation and rotation in the 3D approach and also the wear and the shape in the 2D one.

Finally, the resulting models of rail pieces are put together, and they are adjusted to a smooth curve representing the rail axis. The final model is then outputted to a usable format and a validation process is performed to test how the result fits the original point cloud.

3.2.   A parametric rail model

In order to impose the required constraints a parametric rail model has been designed to reconstruct the rails. The advantage of this model is that it represents the geometry of the real rail preserving representative geometrical properties of the object, such as the angles between the different elements of the object, or the distance between opposite faces.

If compared to real rails, the models developed during the research are much simpler, using rectangular angles between their faces, and only planes instead of curved surfaces. This approximation simplifies the task of adjusting the model, while the resulting model is still suitable for making measurements and analysing the geometric shape and deformations of the rails.

A note about the coordinate system of the dataset and the model must be risen at this point. Along the document, it is assumed the Z axis is the upward axis of the point cloud. While same assumption is done for the 3D parametric model, in the 2D case, the Y axis has been used as upwards. As for the Y and X axis of the 3D model, they represent the axis of the rail piece and the perpendicular to that axis respectively. The origin of coordinates of the model have been set in the centre of the top edge of the model as can be seen in Figure 5 for the 2D model and in Figure 6 for the 3D case.

Along the document the following convention is followed about the name of the different rotations:

- Orientation: The rotation angle around the model Z axis.

- Slope: The rotation angle around the model X axis.

- Rotation: The rotation angle around the model Y axis.

3.2.1.   Parametric model in 2D

The idea of using a 2D model to reconstruct the rail is that by sweeping such a profile along the rail axis represented by a parametric curve one can obtain a 3D model. Thus, the profile model can be characterized by a set of extrinsic parameters referring to its location and rotation, and a set of intrinsic parameters dependant only on the rail shape that is constant along the object. Additionally, a set of two wear parameters are defined, as they are part of the rail profile description, but they cannot be considered constant along the whole rail.

The extrinsic parameters can be identified as the elements of the transformation matrix required to transfer the ideal model to a real profile in a certain section in the rail. In this case three parameters are identified: the translation along X and Z of the point cloud coordinate system, and rotation around the rail axis. The position of the profile in the rail axis is treated as a known value, whereas the orientation and slope of the rail are unknowns of the parametric curve along which the model should be swept.

As for the intrinsic parameters, Figure 5 describes the following ones:

- Wh: Width of the head,

- Hh: Height of the head,

- Ww: Width of the web,

- Hw: Height of the web,

- Wf: Width of the foot,

- Hf: Height of the foot,

- Hr: Heigth of the wear, the difference between the current head height and its design height,

- Wr: Width of the wear, the difference between the current head width and its design width.
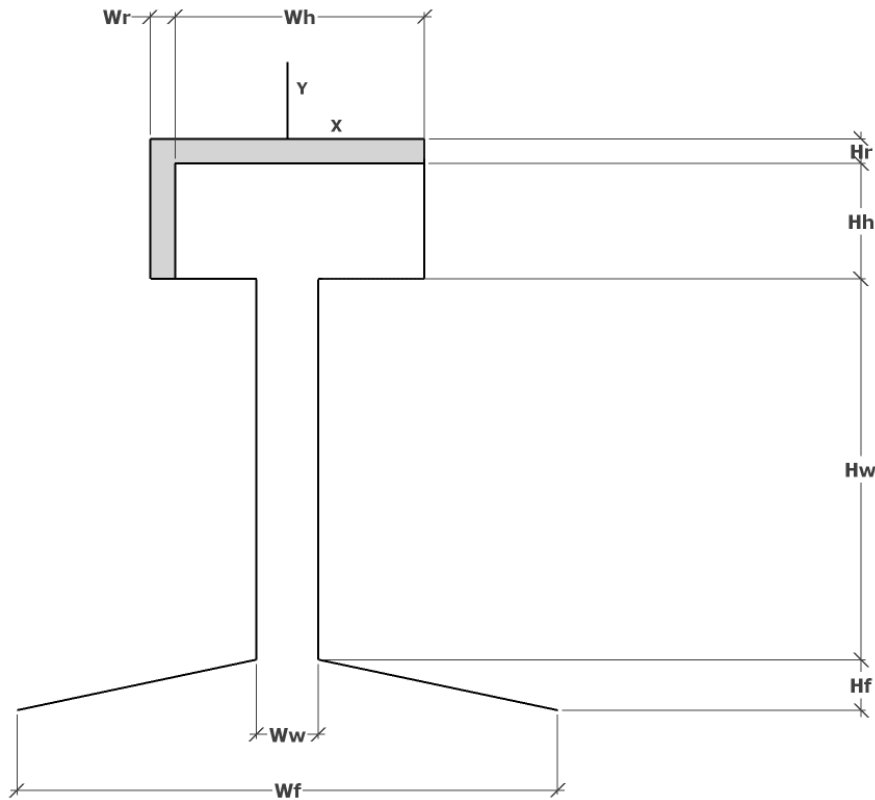
Figure 5: Parametric 2D rail model.

Thus, all the vertices of the model can be defined from the origin of the model coordinate system, set in the middle of the top edge, and using the intrinsic parameters.

Not all these parameters can be estimated at the same time during the fitting step. For example, the height of the web, Hw, cannot be computed due to limitations of the acquisition method, which cannot record any laser point in the bottom plane of the head. Therefore, only the total distance between the top of the head and the top of the foot planes can be adjusted, meaning only one of the components can be treated as an unknown. Similar thing happens with the width of the foot, as its lateral planes can hardly by recovered from the input data; and the same for the width of the web or the head when only one side of the rail has been acquired.

On the other hand, if the design parameters are known, as it is the case (see section 2.1 in page 4), it is only required to solve the model location and orientation by finding the corresponding translation vector and rotation matrix of the model coordinate system with respect to the point cloud one.

In addition to the model and the transformation parameters, two wear parameters have been defined in an attempt to model the erosive effect of the train wheels in the rail over the time. These two parameters are the width wear, Wr, and the height wear, Hr, both relative to the head of the rail. It should be clear that the design height of the head equals the sum of Hh and Hr, as its design width equals the sum of Wh and Wr.

Regarding the orientation of the model, only the angle around the rail axis has been considered. The reason is the other rotation angles are required before slicing the point cloud, in order to perform a correct projection of the points to a 2D plane representing a section perpendicular to the rail axis. Indeed, the difficulty to obtain the orientation by other means is the reason why the 2D method has been dropped in the final methodology in favour of a 3D adjustment. In contrast with the 2D case, a 3D adjustment allows finding the complete rotation matrix at the same time of the other parameters.

3.2.2. Parametric model in 3D

The advantage of a 3D adjustment is the rail piece can be not only located but also completely oriented in the 3 directions of the space. This requires computing the distance between the points in the dataset and the planes of the rail model instead of just lines. Consequently, the requirement for a 3D parametric model arises.

The idea is that in small lengths a rail section can be successfully represented by a straight piece of rail. This assumption seems acceptable as train rails have a radius of curvature which may not be smaller than a design minimum, for safety reasons and dependant on the maximum speed. Thus, the curves on them are smooth with no sharp turns at all. Even for an urban tram, the minimum radius of curvature is as large as 40 m, and thus the error introduced by such an assumption can be as small as 3 mm in a half meter straight piece.

In a 3D parametric modelling approach, all the extrinsic parameters are adjusted altogether, and thus, translations in X, Y and Z axis, as well as their corresponding rotation angles can be calculated.

With respect to the intrinsic parameters, in Figure 6 the following ones are presented:

- Wh: Width of the head,
- Hh: Height of the head,
- Ww: Width of the web,
- Hw: Height of the web,
- Wf: Width of the foot,
- Hf: Height of the foot,
- L: Length of the rail piece.

These intrinsic parameters are known for every type of rail, and therefore they can be treated as constants once the rail type has been set, because of previous knowledge, or by previously trying to fit different types and choosing the one with the best results. Only L is not a design parameter, but it can be treated also as a constant as it is the input length used for sectioning.

All the vertices in the model can then be defined from the origin of the model coordinate system, set in the middle of the top front edge, using the intrinsic parameters defined in the figure.
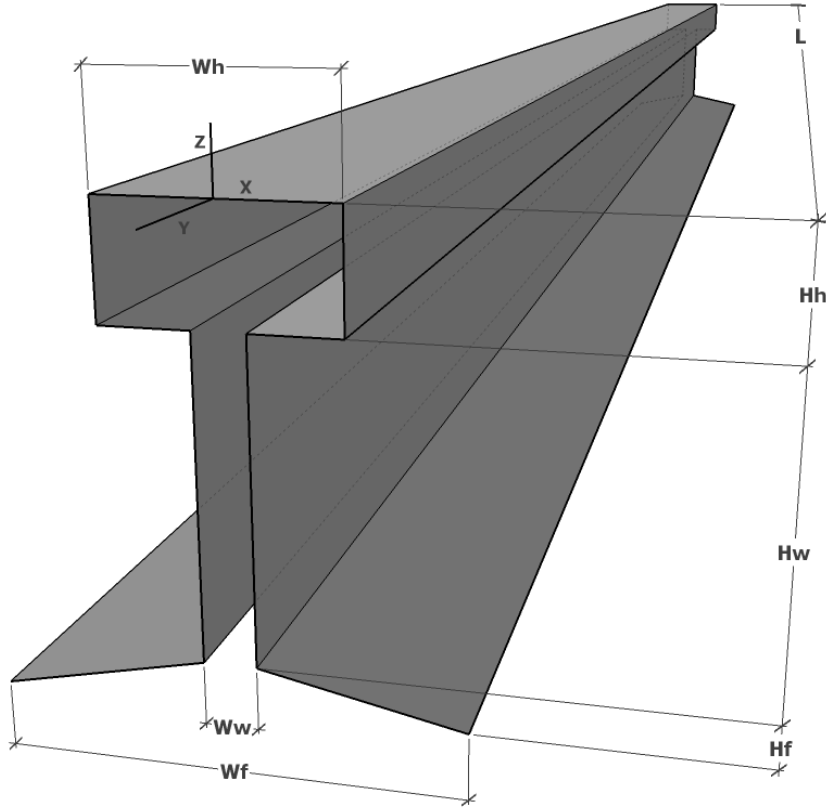
Figure 6: Parametric 3D rail model.

Comparing to the 2D model, only the L parameter has been introduced, to represent the length of the rail piece. This length is not relative to any predesign dimension but instead it depends on the sectioning process of the point cloud (see Section 3.3, Point cloud sectioning, page 12).

In the 3D space, the transformation matrix of the model coordinate system with respect to the point cloud coordinate system, is defined by a t_{xyz} translation vector and the r_x, r_y and r_z rotation angles, representing the rotation around X, Y and Z respectively, which can be used to construct a rotation matrix. Therefore, the transformation matrix, which indeed represents the extrinsic parameters, will be:

$$T = \begin{bmatrix} \cos(r_y)\cos(r_z) & -\cos(r_x)\sin(r_z)+\sin(r_x)\sin(r_y)\cos(r_z) & \sin(r_x)\sin(r_z)+\cos(r_x)\sin(r_y)\cos(r_z) & t_x \\ \cos(r_y)\sin(r_z) & \cos(r_x)\cos(r_z)+\sin(r_x)\sin(r_y)\sin(r_z) & -\sin(r_x)\cos(r_z)+\cos(r_x)\sin(r_y)\sin(r_z) & t_y \\ -\sin(r_y) & \sin(r_x)\cos(r_y) & \cos(r_x)\cos(r_y) & t_z \end{bmatrix} \quad (1)$$

It should be noted these rotation parameters are relative to the model coordinate system and not to that one of the dataset.

3.3.   Point cloud sectioning

The input point cloud data, whether it is obtained manually or automatically, is processed to crop the points of the individual rail that is going to be reconstructed.

As the parametric model is polyhedral, in the sense it has flat faces and straight edges, a technique to progressively adapt to track curvature and slope changes is required. For this initial approach to the problem, a solution involving the adjustment of small pieces of rail to the point cloud has been implemented, which avoids having to deal with more complex curved models.

For further processing, the rail pieces are required to be approximately rectangular. Therefore, to generate the sections an idea of the orientation of the rail with respect the X and Y plane is required. In areas with strong curvatures a progressive orientation dependant on the section would be required.

The sectioning or slicing process is done in pieces of equal length. This length is dependent on the point cloud density and the curvature and slope of the rails. It should be noted that lower point densities require larger pieces in order to provide enough points for a robust fitting, whereas, the higher the curvature in the track, the smaller the pieces should be to adequately represent the rail.

The maximum introduced error in the distance between the rail and the model because of a straight piece not fitting to a curved rail can be found by the following formula:

$$e = r - \sqrt{r^2 - l^2} \quad (2)$$

where e represents the maximum introduced error, r is the minimum radius of curvature of the rail track, and l is the length of the rail pieces as expressed in Figure 7.
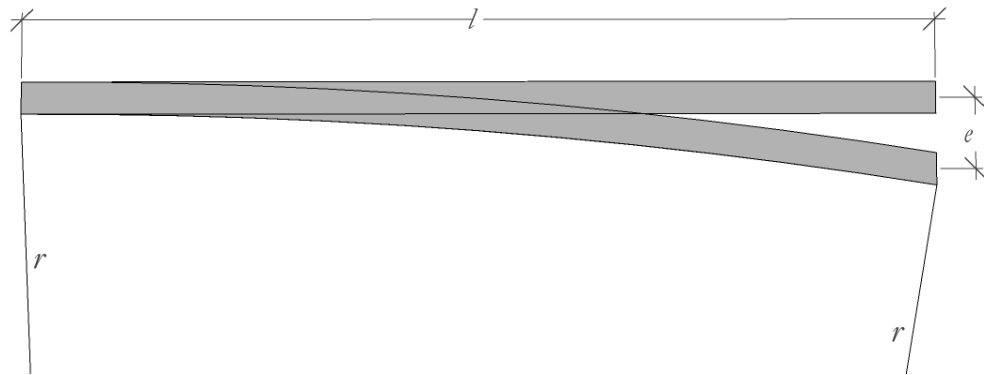
Figure 7: Error e introduced for a radius r rail because of straight rail assumption.

In the following chapters the effect of the length in the least squares convergence rate would be discussed, because a larger length implies a larger number of observations.

3.4. Approximation of initial values

The least squares adjustment method used to fit the model require a set of initial values for the parameters of the model, as the system is non-linear and should be solved iteratively. This is a critical step as it can largely influence the result of the next phases. Different operations have been used for each parameter as explained in the next paragraphs.

3.4.1. Translation parameters

The minimum Y coordinate and the maximum Z coordinate among all the points in the rail piece have been selected respectively as initial Y and Z translation values.

To calculate the initial X value, the points in the head of the rail are selected and then the mean X has been accepted as an initial value for the translation along the X axis. For the purpose of selecting all the points of the head, the points contained within a 5 cm buffer around the plane located in the Z initial

value have been considered as part of the head. This buffer threshold can be adjusted depending on the head height design and the point cloud noise factor. This initial X value would be more accurate when the distribution of the points in the head along the X axis fits better to a symmetrical distribution.

3.4.2. Rotation parameters

The rotation around the X and Y axis is initialized at 0 radians. With respect to the rotation around the Z axis, the orientation of the railway track is taken as input when it is known, as it is the case in straight rails where a Hough Transform has been used to detect the rail points (Arastounia, 2012). In cases where the orientation is not known, the parameter can be approximated using the rail piece point cloud extend. The angle is thus obtained by using the arctangent of the X extent divided by the Y extent, which is the angle formed by the diagonal of the rail piece.

3.4.3. Wear parameters

The initial value for the wear parameters, the difference between the real rail measures and the design dimensions, are simply set at 0, as the initial hypothesis is no representative erosion has happened.

3.5. Detection and handling of outliers

Due to the uncertainty in the laser observations the points' location has an inherent error dependant on the acquisition method. As the results of the fitting method introduced by this research is dependent on the accuracy of the input observations, some pre-processing of the data is required in order to limit the cases where filtering and convergence of the model to the point cloud can fail.

To detect the outliers, first of all the points are projected into the XZ plane using the principal component analysis and ignoring the resulting value of the main axis coordinates, this is the Y axis of the model. Then, the observations out of a reasonable range are erased from the set of points being considered to reconstruct the rail.

3.5.1. Principal components analysis

The principal component analysis (PCA) method simplifies the information of the point cloud by correlating the coordinates of all the observations analysed within it (Smith, 2002). As a result three vectors are found indicating the main directions of the point cloud. Corresponding to each direction is a value that expresses the variation of the points in that direction. These are indeed the three eigenvectors and the three eigenvalues of the covariance matrix of all mean-centred point coordinates.

A new coordinate system is then defined that constitutes indeed a vector space for which the 3 calculated eigenvectors are a basis. The new coordinate system has the property of differing from the model coordinate system only by a translation transformation. In this case the axis defined by the eigenvector corresponding to the largest eigenvalue corresponds with the Y axis of the model, whereas the second and third eigenvectors will correspond to the X and Z axis in the model coordinate system. This can change depending on the length of the rail pieces and their height. For example, if not only the head points are used as input, the smallest eigenvalue will correspond to the X axis.

3.5.2. Interquartile range criterion

In order to improve the results of the filtering method, all the points not close to the surface of the rail head are outliers and should be ideally removed to avoid failure during the filtering operation. Thus, points with an X value, in the new coordinate system, outside 1.5 times the interquartile range, are considered outliers with respect the lateral planes of the head, and are consequently removed from the observations matrix. This procedure is repeated for the new Z axis, but only after the correspondence

step, and only for the points identified as part of the top plane, so vertical outliers can be also removed before the fitting phase.

The interquartile range criterion is preferred to other statistical methods based on the mean and the standard deviation. The reason is those stats can be biased by the outliers while the interquartile range is not, because it is based on frequency of appearance of the observed values. Thus being centred on the median, it is more suitable to know what observations are extreme in contrast with the great majority laying on the rail.

3.6.   Establishing point to plane correspondences

One of the biggest challenges when running a least squares adjustment is to decide in which plane lays every point, as the equation required for every point varies depending on the plane. Therefore three different methods have been considered for this pre-fitting step.

3.6.1.   Manual assignment

The simplest way is to manually decide to which plane corresponds each point. Although this is a straightforward method, it is not oblivious to mismatching due to a poor visual interpretation of the location of the rail piece by the operator. Additionally, it involves a considerably large amount of work specially when dealing with large datasets. Therefore, this method has been used only during the first stages of the research, and has been involved only in obtaining the 2D fitting results.

3.6.2.   Orthogonal distance

The second method attempted is by computing the orthogonal distance of each point to each plane of the model. Then, the nearest plane to the point is considered to be the corresponding one. The main problem in this case is that the approach depends on the initial values used to position and orientate the model.

An improved version of this method considers, in addition to the orthogonal distance, the projection of the points inside the boundaries of the planes. However, this method is also largely dependent on the initial approximation of unknown parameters.

3.6.3.   Point filtering

Finally, a method has been developed consisting into determining the correspondence for the points of the head depending on their relative position with respect the rest of the points in the point cloud.

In a first step a structuring element is defined similar to that used in DTM ground filtering operations. This structuring element is placed over each point in the dataset section, and it is checked if any other point in its range lies above it. If no other point is found, then the point is selected as part of the top plane of the head. This process is illustrated in the left image of Figure 8, where three points are found above the structuring element.
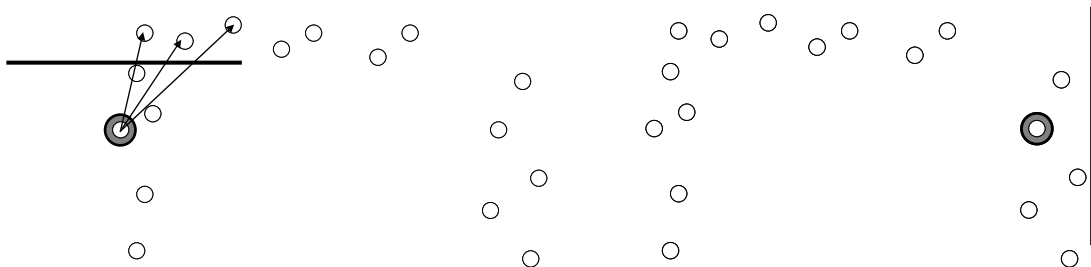
Figure 8: The point in the left image is not detected as part of top plane as it has points above its structuring element. In right image the point is detected in the right plane as no other points are to the right of its structuring element.

For the lateral points the same operation is repeated, but this time the structuring element is placed over the point in vertical position and the points to the left are checked when finding the left plane, whereas the right ones are checked when finding the right plane. Only the points located within a buffer equal to the height of the head from the top plane are considered as candidates to be part of the lateral planes.

The structuring element is placed within a distance of the point to be checked equivalent to the laser measurement uncertainty, and a factor relative to the structuring element dimensions and the rail orientation. In this case a structuring element of 20 cm by 20 cm and a distance threshold of 1.5 cm have been used. These factors have been successfully tested with orientation angles of the rail axis around the Z axis smaller than 20º.

It should be noted the fact that after labelling the points as part of one plane, they are no longer considered as candidates when searching for subsequent planes.

3.7.   Rail piece model fitting

Three different methods have been considered in order to fit the rail model to the dataset. First of all, a 2D adjustment where the model is defined by the bounding lines of the rail piece. Next, two methods have been explored in order to adjust the model in 3D, facing different problems and opening new opportunities.

3.7.1.   2D non-linear least squares adjustment

This method exploits the idea of having a set of thin slices of rail point cloud that are used to orient a 2D profile. Thus, in addition to the model parameters, a rotation factor around the rail axis is defined, and the resulting set of profiles progressively can adapt to the rail curvature.

A 2D model is defined as expressed in section 3.2.1 (page 9). Then a least squares adjustment is used to minimize the algebraic distance of each point to its corresponding edge. The input equations are therefore the implicit formula of a line using as X and Y the coordinates of the correspondent point. A first grade Taylor expansion is used to linearize the equations at the point defined by the parameters of the model. After the observation matrix is built, the equation is solved, obtaining as a result and approximation of the gradient for each parameter that should be added to the actual values in order to converge to a better solution. The initial parameters calculated in a previous step are used firstly, while the updated parameters after the iteration are used for the next one.

The iteration is stopped when the parameters converge into one solution, that is, the gradient is smaller than a certain threshold, in this case 0.001 m or radians. Otherwise, after 20 iterations the process is considered not converging and the iteration is stopped.

This method requires high density input data, in order to have enough observations in the thin slices. As the slices are thin, it is assumed that they can progressively adapt to the changes in orientation of the rail.

3.7.2.   3D non-linear least squares adjustment

This method is equivalent to the previous one, but plane instead of line implicit formulas are used. As a result more points can be used, as the pieces are larger in this case, ranging from 0.5 m to 10 m length. This makes the estimation more robust. A detailed explanation about least squares adjustment of plane surfaces with respect to laser point clouds can be found at Rabbani (2006).

3.7.3.   3D linear model using singular value decomposition

The estimation model can be made linear by considering the rotation matrix elements as independent factors, thus not forcing the rotation matrix to be orthogonal. Then, the distance between the points and

their corresponding planes can be minimized in order to estimate the transformation parameters (Sande, Soudarissanane, & Khoshelham, 2010). This is done by solving the following equation:

$$N \times H \times P = 0 \quad (3)$$

where $\times$ stands for matrix multiplication, N contains the plane parameters, consisting of unit normal vectors and distance to the origin d, H is the transformation matrix, and P contains the coordinates of the points. The equation can be developed as follows for a point j laying in plane i, being $j = 1, 2, …, n$ the set of points in the point cloud, and $i = 1, 2, …, m$ the planes of the model:

$$\begin{bmatrix} n_x & n_y & n_z & d \end{bmatrix} \times \begin{bmatrix} r_{11} & r_{12} & r_{13} & t_x \\ r_{21} & r_{22} & r_{23} & t_y \\ r_{31} & r_{32} & r_{33} & t_z \\ 0 & 0 & 0 & 1 \end{bmatrix} \times \begin{bmatrix} p_x \\ p_y \\ p_z \\ 1 \end{bmatrix} = 0 \quad (4)$$

where the normal of a plane is (n_x, n_y, n_z) and d is the orthogonal distance from the origin to the plane, the coordinates of a point are $(p_x, p_y, p_z, 1)$, r are the elements of the rotation matrix and t those of the translation vector.

After the transformation matrix H is found, the rotation matrix is made orthogonal. For this purpose, the rotation matrix is decomposed using the singular value decomposition method, and the matrix of singular values is forced to be an identity matrix. Finally, it is checked whether the resulting matrix is a true rotation or a reflexion, and in the latter case it is converted to a rotation matrix.

3.8.   Curve fitting to reconstructed rail pieces

After the model pieces are reconstructed for several sections of the data, they must be connected smoothly and adjusted to the track axis using a curve model.

3.8.1.   Bezier curves fitting

Non-rational Bezier curves were chosen to fit the edges of the rail as they are invariant to transformation (Campbell, 2012). These curves require a set of control points that define the constraints to smooth the curve. The midpoint of each of the 4 edges that comprise the head of the rail pieces have been used as control points.

As the curves are described in 3D, a 3rd degree non-rational Bezier curve has been used. Between every pair of control points, a set of f points has been calculated to represent the curve. The resulting number of points is equivalent to multiply the number of control points by f. This factor depends on the expected resulting smoothness, and it must be bigger when using large rail pieces than with small ones.

The following formula describes a Bezier curve:

$$C(u) = \sum_{i=0}^{n} B_{i,n}(u) P_i \quad (5)$$

where n is the number of control points, $C(u)$ is the curve point at u, and u is the curve parameter incremented from 0 to 1 by steps of $1/(fn)$, B_i a blending function and P_i the corresponding control point. The blending function is defined by the Bernstein polynomials, where i corresponds to the iteration number:

$$B_{i,n} = \frac{n!}{i!(n-i)!} u^i (1-u)^{n-i} \quad (6)$$

Although the initial approach was to take the vertex of the rail pieces edges as control points in order to reconstruct these edges with curves, the distance constraint between those edges showed to be not preserved in the initial tests.

In order to model the rail curvature while preserving the rail profile constraints, a different method consisting of a 6th degree non-rational Bezier curve to adjust the rail pieces extrinsic parameters was developed. In this case, every control point has six dimensions corresponding to the translation along the three axis and the three rotation angles around them. Consequently the result of $C(u)$ is a 6x(fn) matrix where every column can be understood as the parameters of a rail profile that can be reconstructed using the 3D rail piece parametric model. The result is a set of profiles that not only are located and orientated smoothly with respect to their neighbours, but also preserve the rail constraints implicit in the rail model. Careful attention must be paid in the angular parameters, as 360º and 0º are equivalent angles but do not generate equivalent results.

One interesting property of the Bezier curves approach is the sections of the rail with gaps, due to rail pieces unachieved fitting or ignored extreme results, are automatically filled with intermediate profiles dependant on the surrounding rail pieces.

3.8.2. Surface reconstruction

Finally, the rail surface can be modelled by closing the boundary of the rail connecting the equivalent vertices of each profile and its direct neighbours. Every surface is delimited then by two profiles and two edges and can be defined by their four corresponding vertices. The problem is those four vertices are no longer coplanar because the profiles have different rotations due to the rail deformations. This results in a curved surface that can be approximated using triangular planes, if it is assumed that the distance between the rail profiles is small in comparison with the deformations in the rail surface.

Therefore, each of the nine faces delimited by every pair of profiles is approximated by two triangular planes. The smaller the separation between profiles, the smaller is the difference between the triangle planes and the curved surface, and the more accurately the model represents the real rail. Therefore, the quality of the resulting model depends on the length of the rail pieces used for fitting and the parameter f that controls the number of profiles per piece in the Bezier adjustment, because given a rail section the more profiles used to approximate the curvature, the short the distance between them.

3.9. Validation procedure

In order to validate the piece fitting methodology it is possible to use the residuals of the least square adjustment for each of the pieces. Nevertheless, a different method is required to validate the final Bezier rail model so the effect of the curvature adjustment is included in the assessment. Hence, a method to compute the distance from all the points of the rail to the nearest plane of the Bezier rail model has been developed. Even if the point cloud is limited by its own accuracy it is still the best reference available from the real rail. The distance computation proposed represents not only the differences between the rail and the model, but also the noise in the dataset and the misclassifications in the rail detection process, and can be consequently seen as an assessment of the complete method.

3.9.1. Distance from a point to a finite 3D triangle

The distance from a point to a plane can be computed as its orthogonal distance. Nevertheless, in this case the planes are finite triangles, and the orthogonal distance is not always a representative characteristic of the separation between a point and a triangle. Therefore for validation purposes, the orthogonal distance has been accepted as the distance only when the orthogonal projection of the point to the plane lay inside the finite triangle. In the rest of the cases, the distance to the nearest edge is accepted as the distance

between the point and the triangle. Thus, in order to know if the point projection is inside the triangle a test has to be executed before deciding which distance should be computed.

Considering the tetrahedron formed by connecting the vertices of the triangle to the point, the projection of the point to the plane of the triangle would be inside the triangle, if, and only if, the angle formed by the plane of the triangle and the faces that have the point as a vertex are acute. This is illustrated in Figure 9, where left tetrahedron P faces have and acute angle respect the ABC triangle, while in the right one, this is not true for the face PBC, and the point P is consequently outside the base triangle.
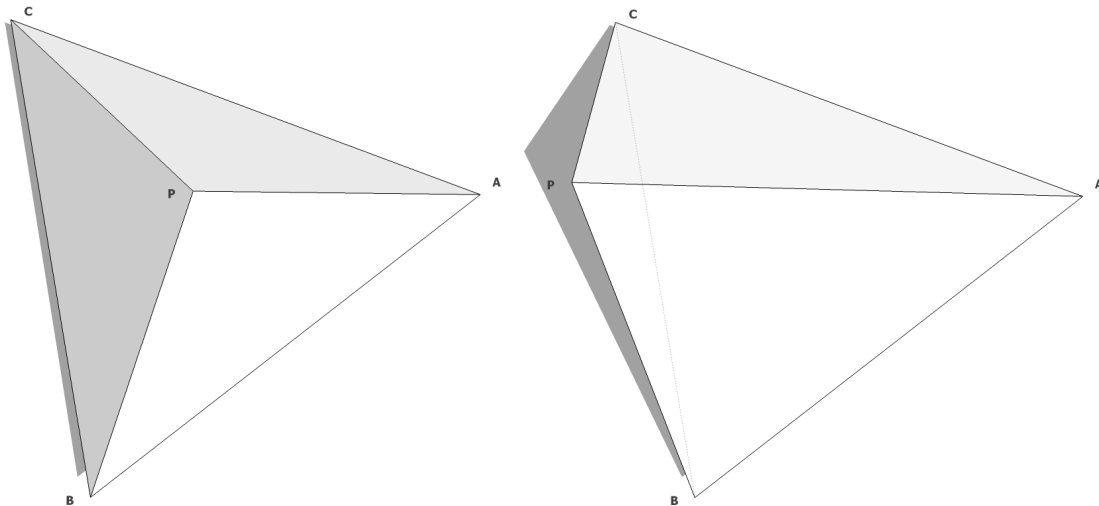
Figure 9: Tetrahedron formed by a triangle plane and one point. In left image the point P projection in the plane is inside the triangle, while in the right, it is outside.

The angle between two planes, the faces of the tetrahedron in this case, can be found from the angle formed by their normal vectors. Thus, in a right handed system the two faces will form and acute angle when their normal vectors are obtuse, as shown in Figure 10.
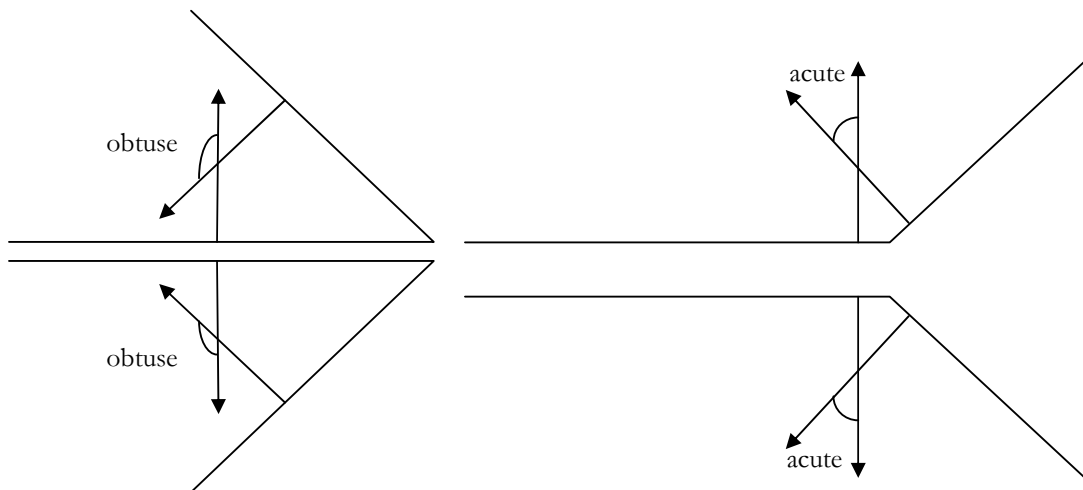
Figure 10: Relationship between faces angles and their normal vector angles.

There is a relevant property of the dot product that allows to test if the angle θ formed by two vectors u and v is acute or obtuse (Anton, 1994):

- θ is acute if and only if $u \cdot v > 0$

- θ is obtuse if and only if $u \cdot v < 0$

- θ is rectangular if and only if $u \cdot v = 0$

In order to be comparable for this application, these normals should be computed consistently, using vectors pointing to the same plane sides respect the segment they share in common. This can be done by computing the cross product of each face, but using in different order the vectors with a common vertex, so the normal of the two planes would be computed as follows (see Figure 11):

$$N_{ABC} = (\overrightarrow{AC} \times \overrightarrow{AB})$$

$$N_{PCB} = (\overrightarrow{PB} \times \overrightarrow{PC})$$
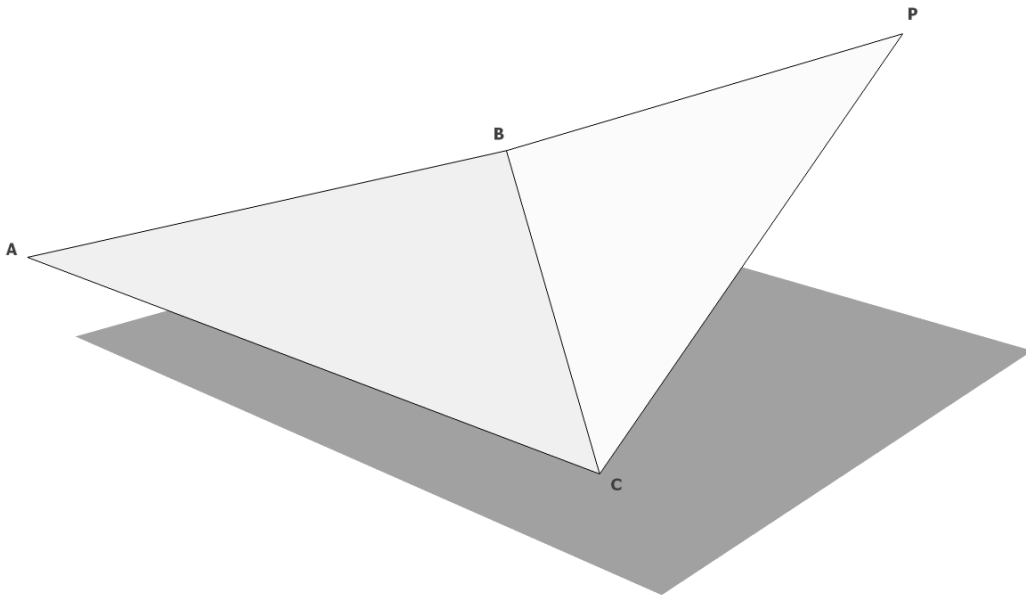
Figure 11: A triangle and the plane formed between a point P and one of the triangle edges, BC.

Then, depending on what faces form obtuse angles with the triangle plane it is possible to distinguish which is the nearest vertex or edge to the point. These conditions are summarized in Figure 12.
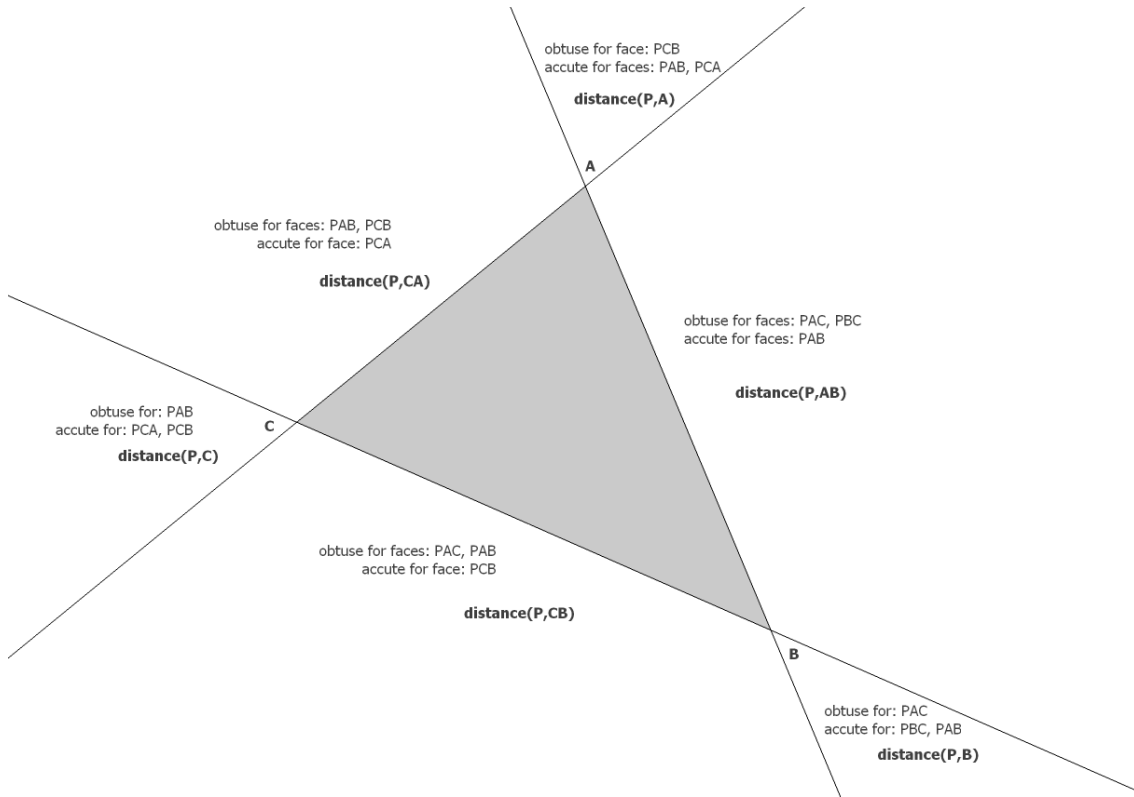
Figure 12: Areas where the point projection can be contained and angular test, labelled by common edge of the triangle and the point face, as well as distance algorithm to be computed in each case.

4.   RESULTS AND ANALYSIS

All the methods have been implemented into a Python program bundled by a common user interface designed with Tkinter. For the statistical and algebraic analysis, numpy module has been used, as well as for reading and writing XYZ plane text files containing the point cloud coordinates. With respect to the visualization of the data and the results, the matplotlib module, and specifically pylab for 2D and pyplot for 3D plots have been used. As for the output format, pycollada bindings to OpenCOLLADA have been selected, corresponding to the .dae file extension.

Whenever manual handling of the data has been done, the PCM software provided by ITC has been used. Finally, SketchUp has been used to visualize and validate the consistency of the .dae output format files.

4.1.   Correctness of correspondences

4.1.1.   Orthogonal distance

The correspondence by orthogonal distance showed relevant limitations. First of all, if the planes are not considered finite, the orthogonal distance to a plane can be small even if the nearest edge is far away from the point. In figure 13, if the web lateral planes are prolonged to the infinite, some points of the top plane are nearer to them than to their actual plane, but as can be seen for the points assigned to 'h' it is an incorrect correspondence as they are more feasibly part of the top plane.
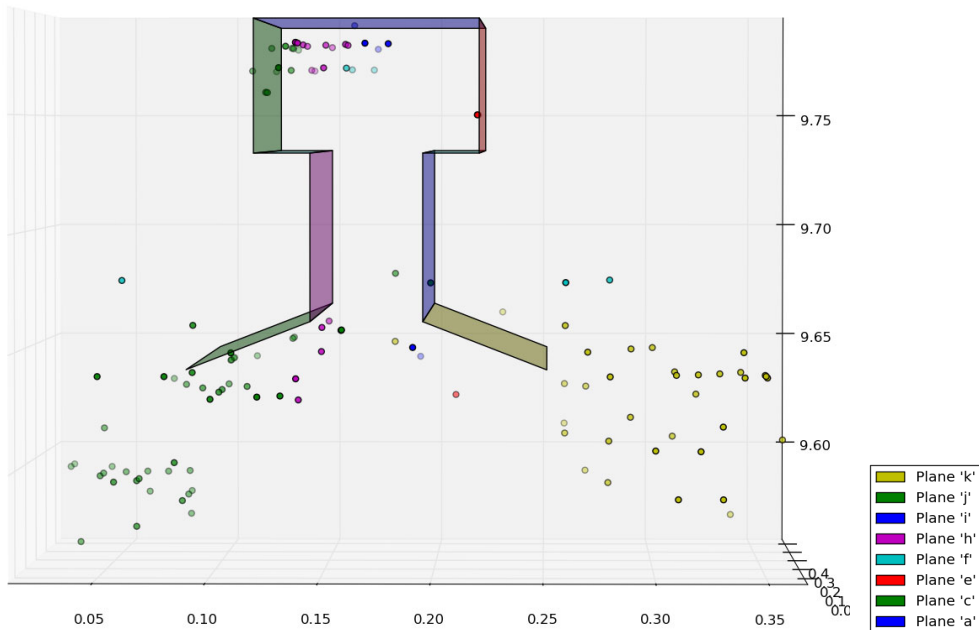
Figure 13: Pure orthogonal distance correspondence.

Even if the planes are considered finite, and the distance to the nearest edge is computed when their orthogonal projection to the plane do not lay into the plane, requiring accurate initial values still remains a limitation. Figure 14 proves the distance from a point to a plane depends on the position and orientation of the model, and thus, of its initial parameter values.
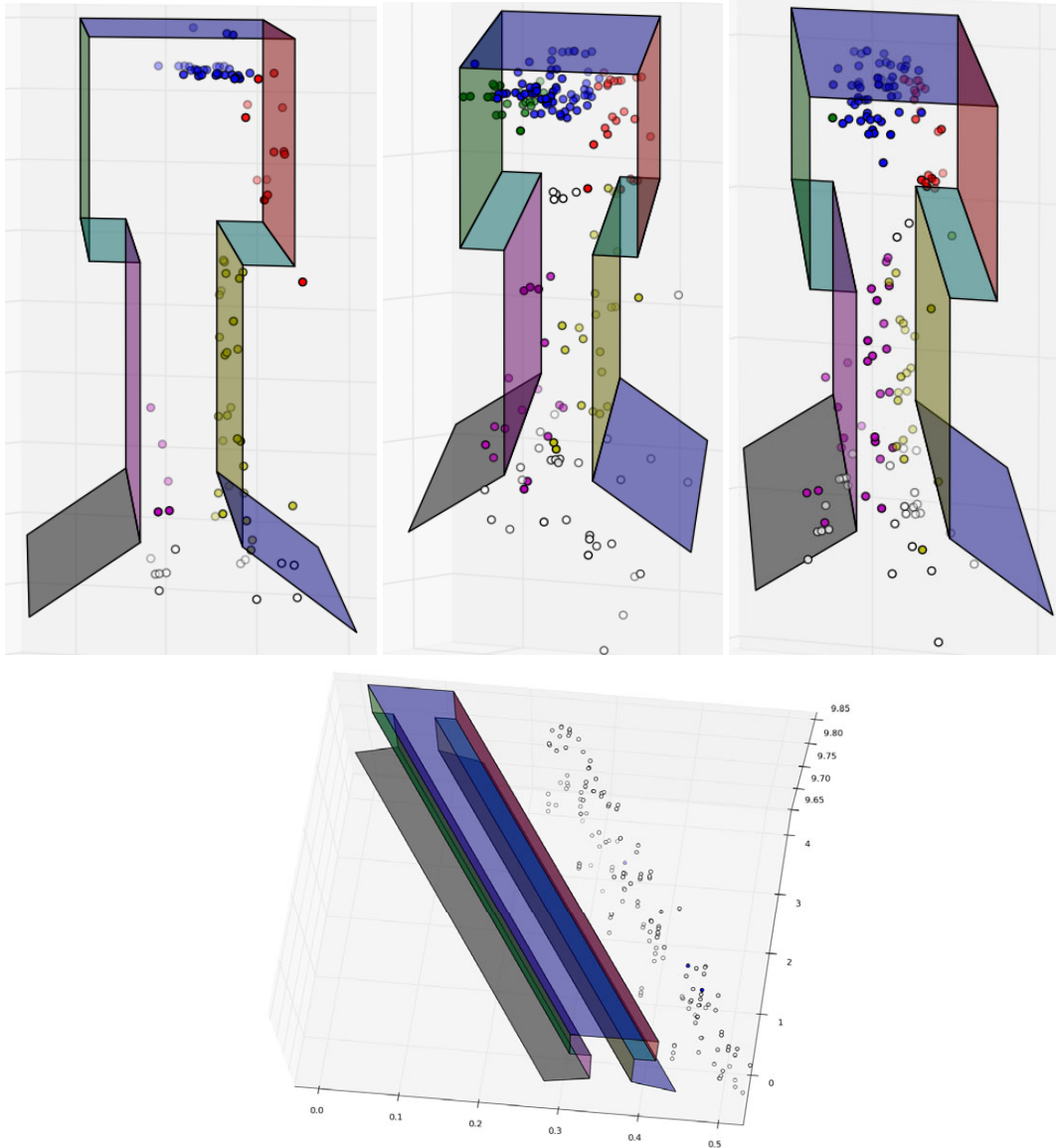
Figure 14: Correspondence by distance with acceptable initial values (left), and not accurate enough initial axis orientation (centre and right). Result with incorrect initial X translation value (bottom).

4.1.2. Point correspondence filtering

Point filtering method was tested against the rails 1 and 2 of the input dataset, using 2 m long rail pieces. Results are presented in Table 1, showing the number of points in the three planes of the head, classified as correct or incorrect depending on whether the automatic correspondence for that point was successful or it was assigned to a wrong plane. In case where a point laying in one plane of the head was not classified, it was counted as non-classified.

The percentage of pieces without incorrect correspondences is over 70% in both side scanned rails, but it fails to just 37% in only one side scanned rails. Whereas the left incorrect values happen just because there are no points in the left and therefore some other points are misclassified, the high rate of right correspondences incorrectness is due to non properly detected outliers. These outliers are maybe produced by reflections, unexpected model shape due to the presence of a joint bar, or registration problems between different scan strips. Whatever the reason, failure to orient the point cloud, as it will be

discussed in this section, makes the implemented statistical outlier detection algorithm not applicable to one side scanned rails, increasing the rate of incorrect correspondences.

One improvement would be not searching for points in one lateral if it is known they have not been acquired. This information can be easily set beforehand, but also automation should be possible by considering the point distribution. For example, once detected the top plane, the mean X value of the top plane when compared to the mean of the whole rail piece, would be deviated towards the side missing the head lateral.

Rail ID	Scan	Piece length	PCA	Correct points			Incorrect points			Non-classified points				Correct_ness	Com_pleteness	No. of pieces	Piece correctness	
				Top	Left	Right	Top	Left	Right	Top	Left	Right	Others				Total	Excluding non-scaned
1	Only right	2 m	Yes	2280	0	1094	13	47	38	23	0	96	1981	97.2%	96.6%	45	37.0%	58.7%
2	Mainly left	2 m	Yes	5267	1402	61	0	5	10	30	35	2	2136	99.8%	99.0%	45	76.1%	-
2	Mainly left	2 m	No	5665	987	40	1	10	14	28	43	6	2136	99.6%	98.9%	45	73.9%	-

NOTE: Points in the corners can be often classified as part of a lateral or top plane, thus the total quantity of top, left and right points can vary between PCA and non-PCA results.

Table 1: Point filtering for plane correspondence results.

Rails number 3 and 4 showed a large amount of correspondence errors due to an unexpected shape; see Figure 15 where points consistently appear in over the top left edge of the rail. Even if from rail 3 it is possible to think that the rail has a different type in this section, from rail 4 it is clear that the problem is in the acquisition method as no train would be able to move in such a rail profile. Because of this reason, the analysis of the results has focused in the track formed by rails 1 and 2.
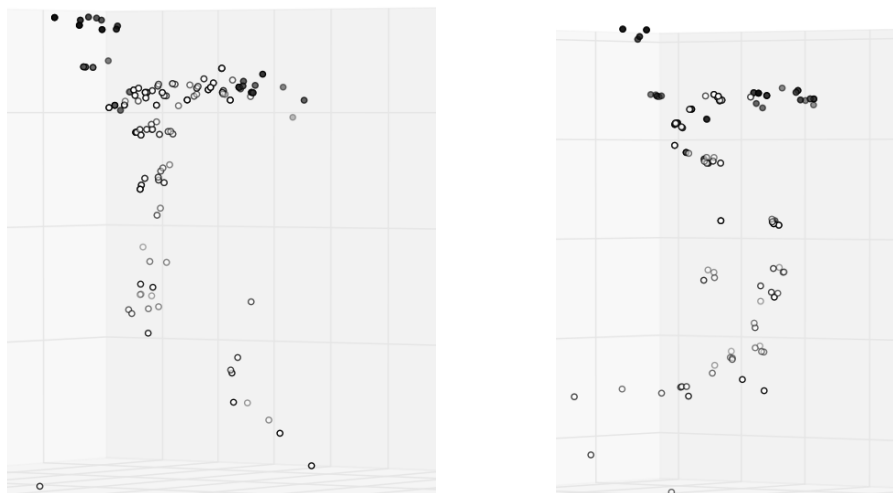
Figure 15: Point cloud shape of rails 3 (left) and 4 (right).

With respect to the outlier detection method implemented, the principal components analysis (PCA), fails when processing only one side scanned rails. In Figure 16, the right lateral of the head was detected as the top plane, 'a', and consequently some points of the right plane, 'e', were detected in what actually was the foot of the rail. The method can establish a relation between the XY coordinates representative of the rail axis, only when the rail axis balance the point cloud, this is, when the correlation of XY is representative of it. Therefore, principal component analysis is not a reliable candidate to retrieve the points coordinates in the model coordinate system when using mobile laser scanning mounted in the same track desired to be scanned, because there are always two laterals of the rail track that are not acquired. Besides this limitation,

the method proved to be useful to improve the filtering of rails scanned in both sides, and thus it has been used to filter rails 2 and 3.
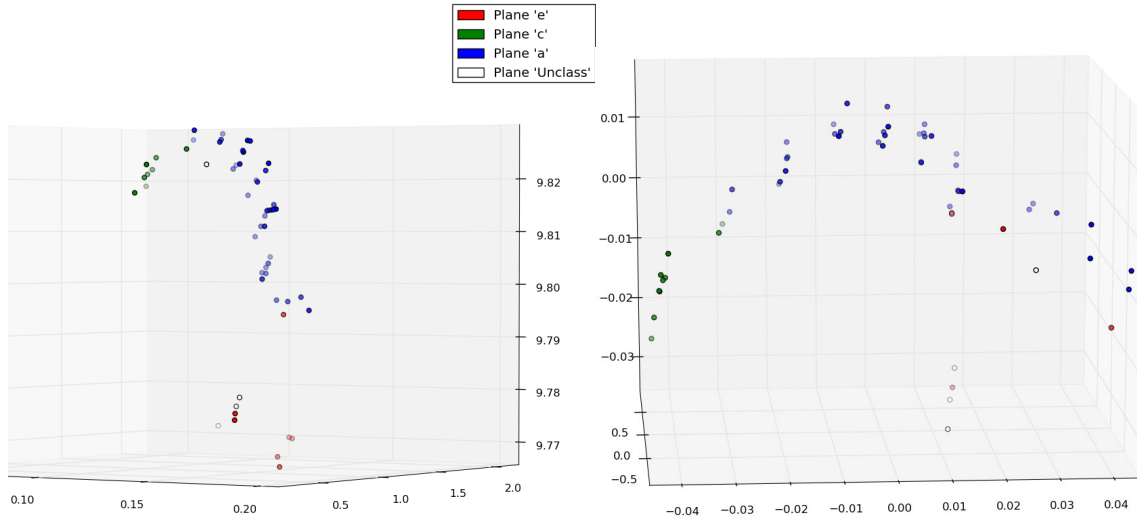
Figure 16: Point cloud in global coordinate system (left) and in PCA coordinate system (right) for an only one side scanned rail piece. The top plane 'a' is detected in the right lateral of the rail.

The incorrect correspondences tend to happen when evaluating the planes with smaller point density. This is, when a point in the top plane fails to be classified, when looking for lateral correspondence is more likely not to find any other point to its side if the point density in that direction is sparse.

Additionally, the incorrect correspondences more often happen in the extremes of the rail pieces. The reason is that in these extremes, the structuring element is projected to a void space where there are no points (indeed they are, but in the next rail piece), thus, halving the filtering success probability.

To avoid this, one possibility would be to execute the filtering before the sectioning in pieces process. The disadvantage would be a higher sensibility to outliers, a larger processing time (unless the point cloud is structured beforehand), and a smaller success rate due to the orientation of the rail. The main point is if the whole rail is not completely straight, principal component analysis will not give a satisfactory result, disallowing lateral outlier detection, and making the filtering susceptible to the orientation because of not using the model coordinate system.

It seems more feasible to additionally consider the previous and the next rail pieces when looking for points beyond the structuring element. Regretfully, this will require the process to work in the same coordinate system, thus, the principal component analysis necessarily will have to succeed in orienting 3 pieces at a time.

With respect to the correspondence problems caused by non-detected outliers, further discussion will follow in section 4.3.3 in page 31, Effect of outliers.

4.2.   Rail piece model fitting results

4.2.1.   2D simulated data

In order to validate the least squares algorithm implemented, a first set of simulated points was created. A pre-set profile was used for this purpose, picking random points situated along the edges of the profile. To avoid this points laying in the edges, a shift factor of maximum 1 cm was randomly introduced in the X coordinate of the generated point.

After setting different initial values for a new profile, the least squares adjustment was performed showing the process was converging into a solution in around 5 iterations (see Figure 17). In this example the model parameters were not constrained and thus, it can be appreciated how the different width and height of the head, web and foot of the rail, were adjusted after each iteration.
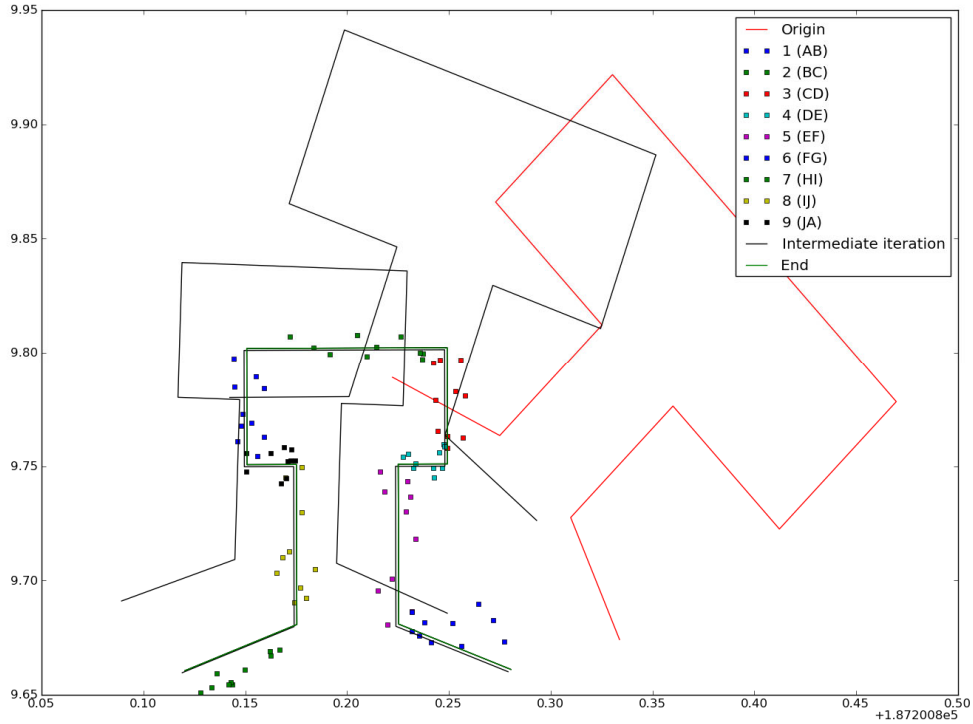
Figure 17: Convergence of 2D model fitting process. Initial profile in red, final one in green.

4.2.2. 2D real data

In order to test the algorithm against real data, the points of one of the rails were manually cropped from the original dataset. The points were manually labelled depending on what planes of the rail they laid. In case it was not feasible to visually identify on what plane they laid, they were assigned the label 0.

Finally, the algorithm was run using different sets of points of the cropped rail. The number of observations in each edge varied from set to set. Should be noted that because an incorrect processing of the input dataset, the results of this 2D adjustment were capped to the cm precision. Nevertheless, the results are still valid to illustrate the advantages, disadvantages and findings of this method.

It was possible to find the 3 extrinsic and 2 wear parameters, see section 3.2.1 in page 9, when at least observations in the following edges were found:

- On top edge (BC), plus on left edge of the head (AB), plus on right edge of the foot (FG).

- On top edge (BC), plus on right edge of the head (CD), plus on left edge of the foot (HI).

- In both of the previous cases, the lateral head edges can be substituted by the web edges.

The name of the edges and the corresponding colour assigned to the points can be seen in Figure 18.
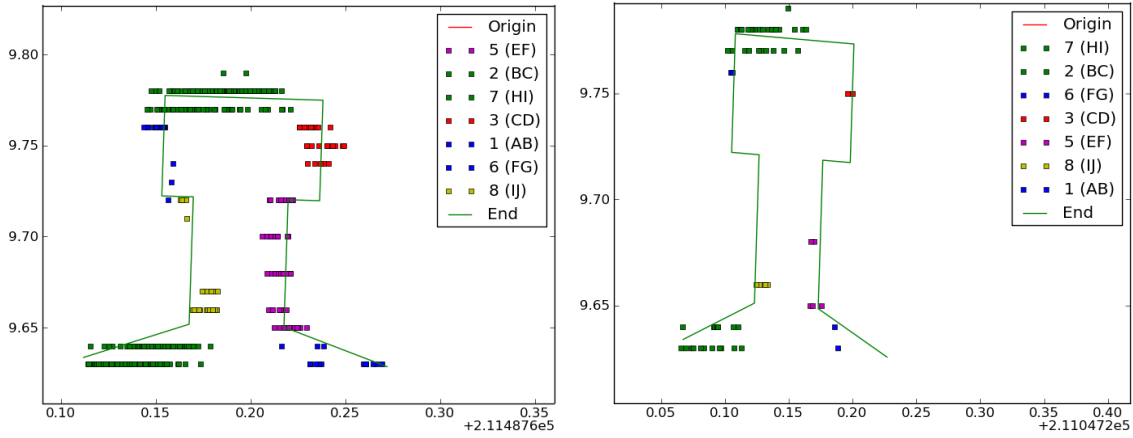
Figure 18: Profile fitting in manually labelled point clouds of 50 m, left, and 0.5 m length, right.

The reason of this requirements is, in first place, to fix the translation in X axis, one lateral edge is required, and a horizontal one for the Y translation. Secondly, at least two points in the same or different edges are necessary to solve the rotation parameter. Finally, the wear parameters require an additional point, after fixing the translation, to be solved. Thus, two points in different horizontal edges are required for the height wear (Hr), and two in different vertical edges are needed for the width wear (Wr).

Because the points in the edges of the foot both constraint the profile in the X and Y axis of the model coordinate system, they can be used as both horizontal and vertical edges, reducing the amount of observations required to solve the system.

Finally, this approach required to project the points to the XY plane. In Figure 18 the hypothesis that the rail was perpendicular to the XY plane was assumed, which resulted in a wrong assumption as can be seen from the points in vertical edges where they clearly line up instead of overlapping. The fact that this line up did not happened vertically in the horizontal edges was an indication that the angle of the slope was near to 0. This makes sense as we know that generally rail orientation variations are more frequent than slope ones.

Thus, this method has the advantage of being able to model the rail wear, and even the rail intrinsic parameters in the case they are not known. The main limitation of the method is the orientation of the rail, and the slope it is high, has to be found beforehand, either if it is manually inputted or it is found by automatic means. To find it automatically, principal component analysis was attempted, reaching new limitations because of the non-symmetry of the observations.

4.2.3. 3D real data and least squares adjustment

The real data was tested using a 3D non-linear least squares adjustment achieving successful convergence in most of the cases. The results are presented in Table 2, where convergence success was considered for any piece that achieved convergence before reaching the maximum number of iterations. On the other hand, adjustment was considered correct when the resulting parameters balanced the model, around the mean, see Figure 19, and the visualization of the model among the rest of the pieces did not show appreciable differences respect the rest of the rail to the naked eye, see Figure 21 in page 29. Finally, the distance in the table refers to the mean distance from all the points in the input point cloud to the final reconstructed model as obtained from the validation of the model, and it will be further discussed in section 4.4 in page 32.

Rail	Piece length (m)	PCA	Nr. of pieces	Convergence success		Correct fitting		Distance (m)	
				Nr.	%	Nr.	%	Mean	Std. dev.
2	0.5	Yes	180	156	87%	124	69%	0.014	0.023
2	1	Yes	90	90	100%	87	97%	0.005	0.005
2	2	Yes	45	45	100%	45	100%	0.005	0.005
2	5	Yes	18	18	100%	18	100%	0.005	0.005
2	10	Yes	9	9	100%	9	100%	0.005	0.005

Table 2: Fitting success and point to model distance.
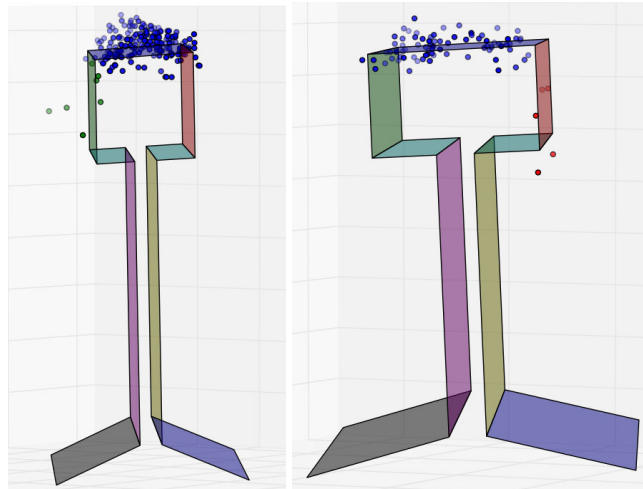
Figure 19: Rail pieces fitting success using filtering and least squares adjustment.

A total of 5 different piece lengths were tested obtaining successful fitting when using pieces of more than 1 m. It should be reminded that the available dataset only contains straight lines, and thus the good results achieved by the 5 and 10 m length pieces more probably will not be successful when trying to fit curved rails. The relation between the proper piece length, the point cloud density and the rail curvature is further discussed in section 4.3.4 in page 31.

Three correspondence methods were tested although only the results for point filtering are presented here. This decision was taken because the initial tests showed the correspondence by distance method was clearly inferior and the manual one was not applicable to the whole dataset because of time constraints. As the only method robust to find correspondences between the foot outliers at this state of the art was the manual one, see Figure 20, only the planes of the head were fitted during the least squares adjustment.
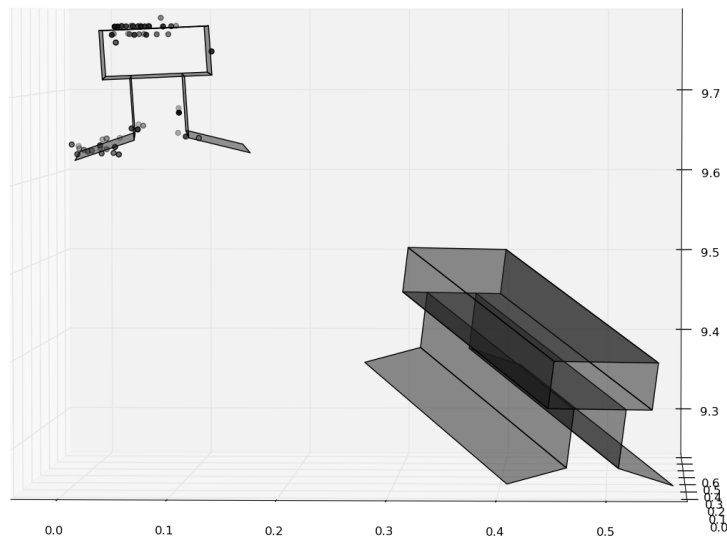
Figure 20: Fitting success, including the initial position of the rail model.

It should be noted that the non-linear least squares adjustment was selected in favour of the one based in singular value decomposition, because it is possible to always find good initial estimates.

4.2.4. Reconstructed pieces visualization

The rail pieces as fitted after the least square adjustment were exported to collada format for visualization. It is clear from Figure 21 that the result using 2 m rail pieces is much more robust than the 0.5 m. The visualization of the other rail lengths analyzed gave similar results to the 2 m one, where the pieces connect one to each other with small variations between them that can hardly be appreciated without zooming in.
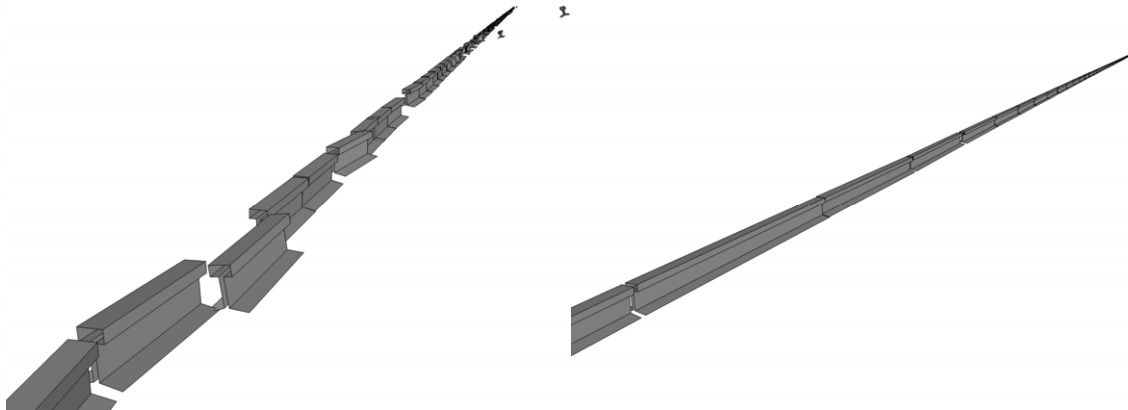
Figure 21: Rail pieces reconstruction with 0.5 m (left) and 2 m (right) length.

4.3. Analysis of the rail pieces fitting process

This section analyses the effect of certain factors in the result of the 3D least squares adjustment. These factors are here presented from more to less impact in the final result of the adjustment.

4.3.1. Effect of correspondences correctness

Failure to properly label the points during the correspondence search process will lead most of the times to a wrong least squares solution. There is a clear difference between failures to classify one point, leading

to a number of observations problem, and wrong classifications. In this last case the least squares usually converges into a wrong solution, Figure 22, or can even fail to find a solution where all the model constraints are preserved.

Depending on the type of correspondence failure, the effect on the final parameters will vary. Orientation incorrectness is related with problems derived from only one side of the rail scanned, whereas outliers shift the piece in one direction.
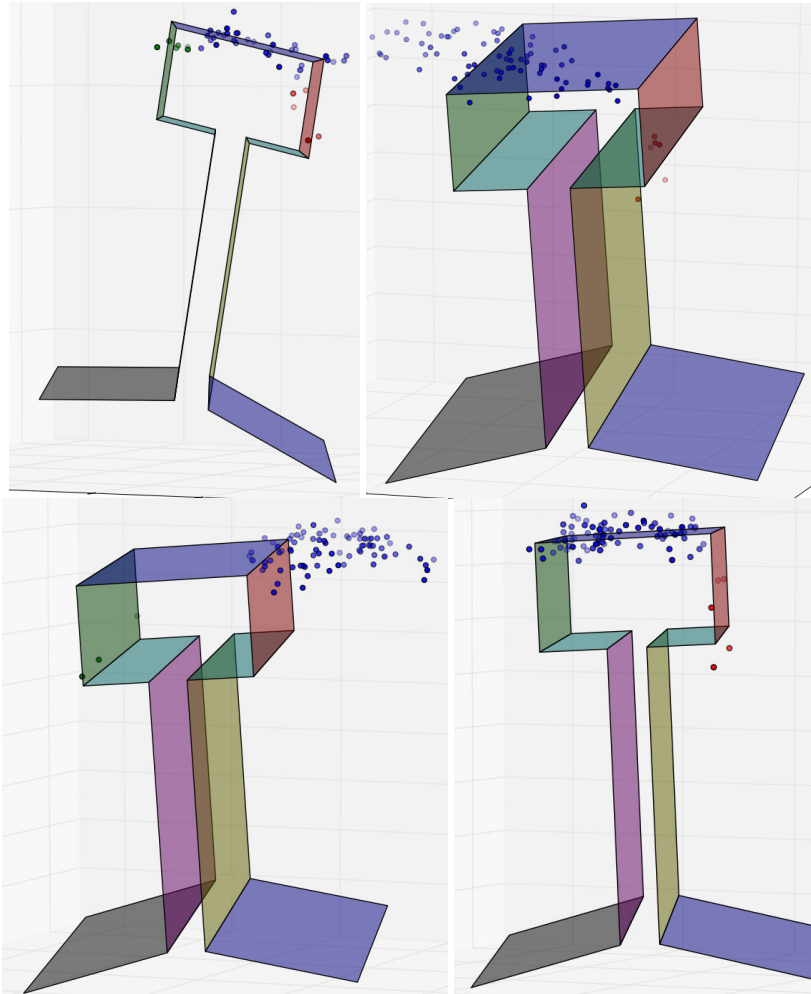
Figure 22: Fitting failure under wrong correspondence (top left), not enough observations (top right), outliers (bottom left), and successful fitting (bottom right).

4.3.2.   Number of observations

The lack of enough observations derives into orientation incorrectness and can even make the equation system unsolvable. In the first case, Figure 22 top right, the filtering process gave a correct result, but there were not enough points to have a good distribution along the piece to ensure the right orientation of the piece faces. The second case, usually occurs when the piece only have points in the top face, or those were the only points that could achieve correspondence.

The number of observations problem is dependant in the piece length and the acquisition method. The shorter the sectioning length, the more probable one of the pieces lacks enough observations to solve the transformation matrix. As about the acquisition method, it influences the distribution of the points along the point cloud, and thus, the density of the points in one of the faces of a rail piece can have not enough

observations. In the analysed dataset the amount of observations in the top face of the pieces is bigger in comparison with the lateral ones; for example, in rail number 2 were found 3.5 times more points in the top face than in both right and left faces of the head summed together, whereas this proportion was reduced to 1.9 in rail 1.

4.3.3. Effect of outliers

Depending on the case, the outliers can affect the fitting process causing incorrect results during the filtering step, or they can cause a shift or wrong orientation during the least squares adjustment, see Figure 23. The effect of outliers in the filtering process produce undesirable point detections beyond the structuring element, consequently removing the point candidate from the set of points laying on the face under check, Figure 23 left.

On the other hand, when an extreme value is still considerably close to the rest of the points in the face and does not lead to a completely wrong correspondence result, there is still the possibility that the fitting result is successful as in Figure 23 right. This happens when the number of observations is big enough to compensate the weight of the outlier in the least squares adjustment. It can seem that higher density point clouds, and larger length pieces can therefore improve the robustness of the fitting process against outliers, but those strategies may introduce a comparable number of outliers with respect to the number of new observations, not improving the results in most of the cases.
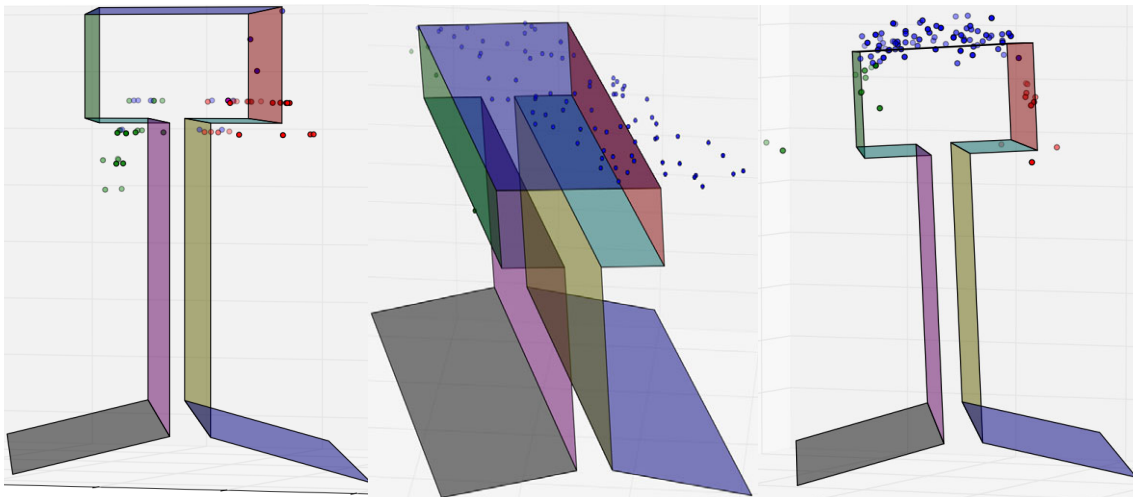
Figure 23: Outliers effect in the filtering (left) and fitting processes (centre), leading to wrong correspondence and orientation respectively. In right image the fitting was successful even with outliers in the left face.

The effect of outliers is considerably reduced when an outlier detection step is introduced before the filtering process. The method used here relies in principal component analysis, which not applicability in only one side scanned rails has been already discussed in section 4.1.2 in page 23.

4.3.4. Effect of piece length

The piece length affects to the number of observations in each piece, thus directly modifying the robustness of the least squares adjustment. The larger the selected length, the more points per slice and consequently the higher the probability the resulting extrinsic parameters of the piece would be representative of the real piece. Additionally, larger pieces have the effect of reducing the number of piece edge incorrect correspondences in the filtering step, as less pieces means less border checks.

On the other side, large pieces may not adjust properly to curvature, slope and torsion of the rail, leading to misrepresentation of the object and higher point to model distances. It has been found that for a

straight rail a good balance between these factors is with lengths of 1 to 2 meters, see Table 2 in page 28. It was not possible to found a similar value in curved rails because there is no such type of rails in the provided dataset.

Finally, it should be noted that pieces with long lengths require less computational time for validation but more filtering time than those with shorter lengths.

4.3.5. Sensitivity to initial values

Whereas it has been already discussed the high relevance of the initial values for the extrinsic parameters of the model when finding correspondences using the distance method, the impact is greatly reduced when using point filtering. Once the importance of the initial values is avoided in the correspondence process, their impact is limited to generally affecting the number of required iterations to achieve an adjustment. Still, when the initial estimation is far away from the real value it is not rare to reach the maximum iterations limit, set to 20 in the discussed implementation, ending in a convergence failure.

4.4. Rail curvature adjustment and final model

4.4.1. Curve fitting result

The adjustment of the top rail edges to two Bezier curves did not preserve the distance between the two curves. Even being Bezier curves invariant to transformations (Campbell, 2012), the curves are not simple shifted copies of each other but independent curves that adapt to different transformations in each of the pieces. It is possible to see the effect in Figure 24 where the left-top edge of the head is plotted in green, the right-top one in blue and the middle curve between them is represented in red. In the figure the Z axis has been magnified so the differences can be appreciated. Nevertheless, the big differences between the two edges are also product of the torsion of the rail, but if the distance between the two curves is calculated for each Bezier point pair, the standard deviation results in 0.002 m, when it should be near 0 if the constraints of the rail model were maintained along the rail.
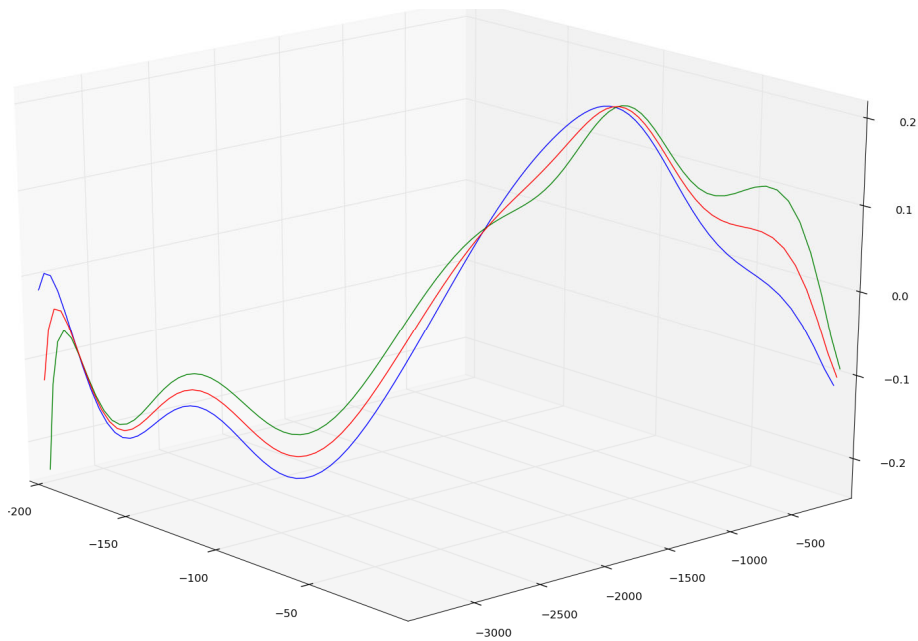
Figure 24: Bezier curves of the reconstructed top rail edges, including control points.

In comparison, the other method implemented by adjusting the extrinsic parameters of each rail piece instead of the vertex of the edges, demonstrated a better behaviour. Being dependant of only one curve in this case, the reconstruction of the rail profiles ensured the maintenance of the distances constraints along the whole rail. In Figure 25 can be observed how all the rail profiles resulting from the Bezier adjustment maintain the model constraints and adapt smoothly the changes in the data. The standard deviation of the distance between the two top edges was consequently 0 m in this case.
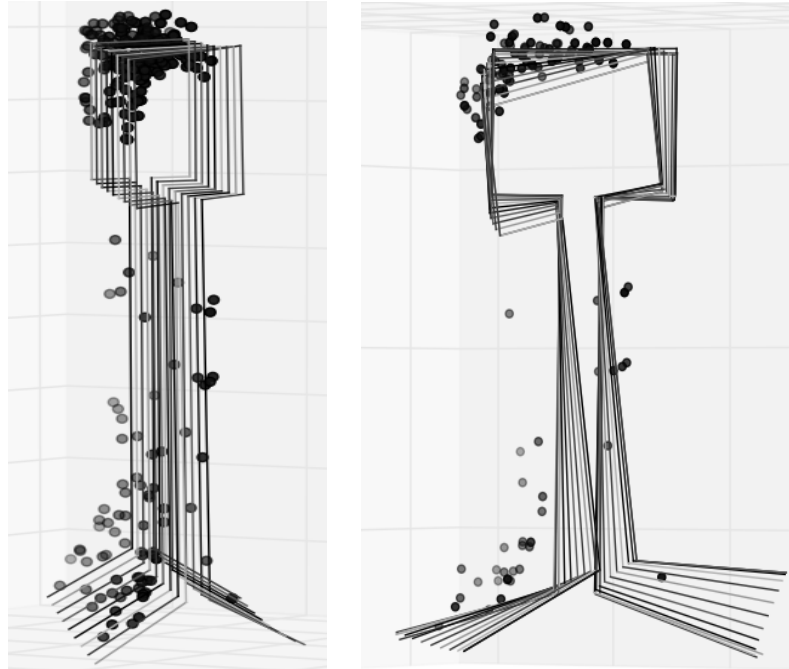
Figure 25: Bezier profile adjustment visualized with the input point cloud.

4.4.2.   Final model visualization

The final model reconstructed connecting the Bezier profiles, was exported to collada format and imported into SketchUp for visualization. The final model showed the complete rail was reconstructed and the changes in the rail rotation were smooth (see Figure 26).
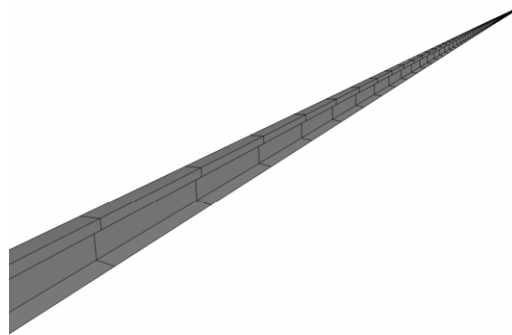
Figure 26: Rail reconstruction using Bezier curves with 3 points per piece and 2 m (right) piece length.

When comparing 0.5 m (left) image of rail piece (Figure 21) with that one of Bezier rail (Figure 26), it is possible to observe how the gaps are filled and the misalignments are interpolated obtaining a smoother

rail. Only the translation errors perpendicular to the rail axis are meaningfully carried over to the final model, in part because those are the largest errors that can be found after the least squares adjustment.

One of the problems when using larger pieces is wrong adjustments brings larger errors in the reconstruction of the rail, as they affect larger sections of it.
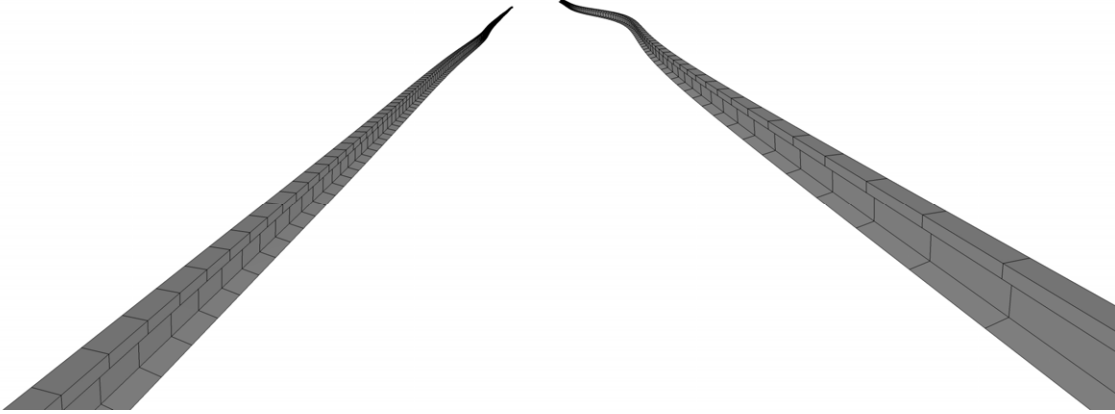
Figure 27: Comparison of the effect of wrong parameters in one piece in 0.5 m (left) and 1 m (right) length. Also demonstration of curves representation in curved rails.

Finally, the four rails in the dataset where put together to obtain a model of the two tracks present in the input dataset (see Figure 3), the result can be seen in Figure 28. Should be noted that even rails 3 and 4 had poor fitting results, with less than 40% of convergence rate, the Bezier adjustment was able to fill most of the gaps, producing a model that if not accurate, at least maybe useful for some visualization applications.
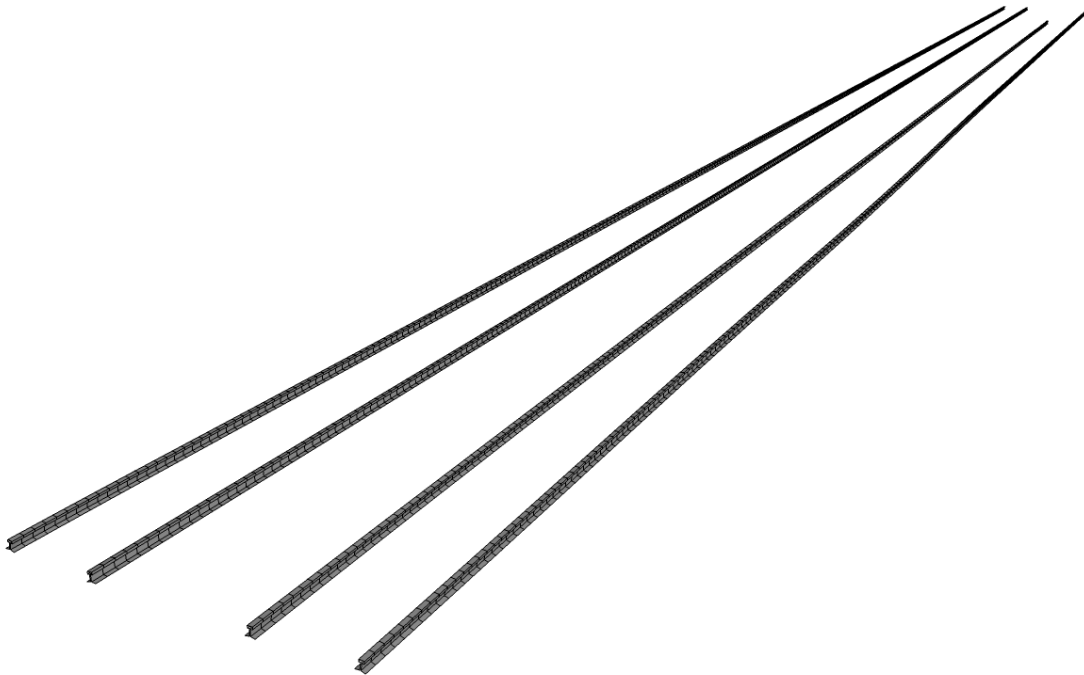
Figure 28: Model of the four rails configuring the two tracks present in the dataset. Rails 3 is incomplete due to fitting of the rail pieces errors.

One limitation of the Bezier curves method is the final curves do not pass through the control points. It is possible then that some deviation from the rail pieces is introduced, although this effect could not be confirmed due to the lack of rails with a considerable curvature in the dataset.

4.5. Final model validation

As a reference model of the reconstructed rail is not available, it was not possible to perform an external validation of the overall modelling process. Nevertheless, an internal accuracy check against the input point cloud can still reveal the quality of the rail reconstruction.

4.5.1. Internal accuracy of the final model

In Table 3 the results of the validation for different experiments is presented. The column notes refers to different options selected while reconstructing the rail, being PCA the cases where principal component analysis was used to detect outliers, and right or left filter when one rail had only one side scanned and the lateral filtering correspondence was applied only to one of the sides. Regarding the distance, it is the geometrical distance to the nearest plane in meters. The percentiles in the table describe the percentage of points below a certain distance. The reason to use percentiles instead of the mean to evaluate the accuracy of the model is because they give a better impression of the distribution in presence of outliers. Nevertheless the mean and standard deviation are also provided. Finally, the percentile at 1 cm states what is the percentage of points that lay at less than that distance to the model, and was used as a measure of quality as it was considered an acceptable accuracy for most of the applications that can follow up the research.

It is remarkable the result of the rail 3, because even being scanned in both sides, it was not possible to reconstruct it completely (see Figure 28), and even the validation method did not consider the points in the no completed area, the results are comparable to those of the lateral rail 1, with only 70% of the points within 1 cm of the model. The reason is this rail has a different shape in the point cloud that does not fit to the UIC 54 model due to some problem in the acquisition system, see Figure 15.

Rail	Notes	Piece length (m)	Distance (m)						
			Mean	Std. dev.	25 percentile	50 percentile	75 percentile	95 percentile	Percentile at 1 cm
1		2	0.008	0.009	0.002	0.005	0.010	0.024	73.9%
1	right filter	2	0.008	0.009	0.002	0.005	0.010	0.024	74.3%
2	PCA	0.5	0.014	0.023	0.002	0.005	0.011	0.076	72.8%
2	PCA	1	0.005	0.005	0.002	0.003	0.006	0.013	90.5%
2		2	0.005	0.005	0.002	0.004	0.007	0.015	86.1%
2	PCA	2	0.005	0.005	0.002	0.004	0.006	0.014	89.0%
2	PCA	5	0.005	0.005	0.002	0.004	0.007	0.014	87.4%
2	PCA	10	0.005	0.005	0.002	0.004	0.007	0.014	86.4%
3		2	0.008	0.008	0.003	0.006	0.012	0.023	69.3%
3	PCA	2	0.008	0.007	0.003	0.006	0.011	0.019	70.2%
4		2	0.009	0.009	0.003	0.007	0.012	0.020	65.0%
4	left filter	2	0.019	0.024	0.003	0.008	0.026	0.072	56.4%

Table 3: Points distance to the model by piece length.

The analysis of the distance from the points to the planes in relation to the piece length used during the reconstruction process confirmed the 1 and 2 m length pieces as the best options to model the rail object. When using these lengths, the percentage of points with less than 1 cm distance to the model is 90%. The rail 2 was used for the analysis of the piece length as it was the rail with a higher correctness (100% of its rail pieces converged correctly). The analysis of the histograms in Figure 29 reveals that the number of points at less than a given distance increases rapidly until the 1 cm.
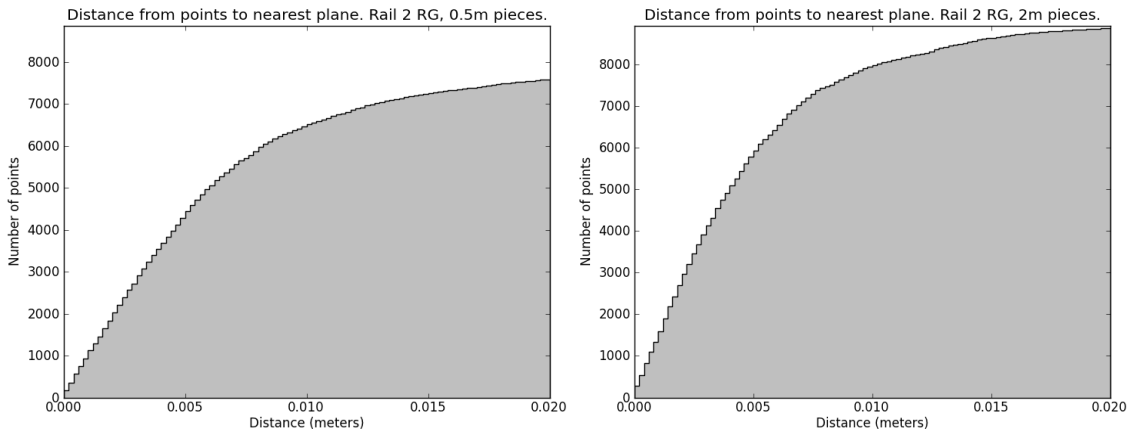
Figure 29: Distance histograms showing the number of points below a certain distance to the model.

Plotting the points in the dataset with different colours depending on the distance to the nearest plane of the model as in Figure 30, revealed the best fitted ones lie on the head, while the distance of the points in the foot is larger. This is understandable as the planes in the head are the ones used for the fitting. It is also indicative of the higher amount of outliers in the bottom part of the rail, probably because of the elements as bolts or ballast laying in this area, but maybe also influenced by the laser incidence angle in this inclined surface. In fact it may be possible to filter the points laying at more than 1 cm from the model to obtain a set of points corresponding to bolts and ballast.
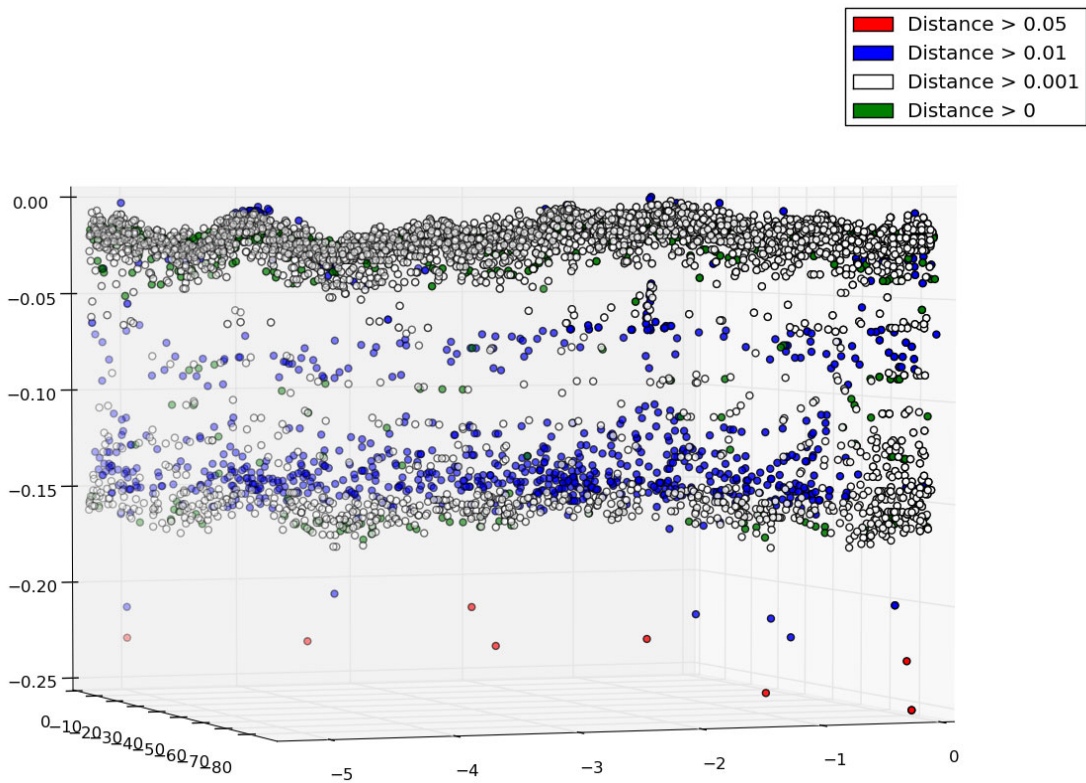
Figure 30: Points classified according to distance to the nearest plane of a model of rail 2 with 2 m length pieces.

One of the problems of this validation process is to which extent the distance from the points to the model is the product of modelling deviations or is a result of the noise in the dataset, whereas it is intrinsic from the laser device or due to registration inaccuracy of the different strips. It may be revealing to validate the model against another dataset with higher precision, for example using a terrestrial laser scanning of part of the rail obtained at the same time of the mobile one.

Additionally, in order to better understand the effect of the Bezier adjustment, calculating the distance between the final model and the fitted rail pieces will be required.

4.6.   Output model format

The final reconstructed model is exported to the COLLADA file format. This format defines an open standard XML schema commonly used to interchange models between 3D modelling software applications. Its files are identified by the .dae extension.

For the final output the patches defined from the Bezier curves are stored as they are, whereas in the case of the rail pieces, only one model is stored and then a translation vector and a rotation matrix are stored for each piece, reducing the file size.

5. CONCLUSIONS

5.1. Summary

A method to automatically model train rails from laser scanning point clouds has been developed. It has been proved that it is possible to generate a curved model from straight rail pieces fitted to the faces of the rail. The fitting result of the rail pieces depends on their length and the success of the correspondence method, which is sensible to outliers. Even if a considerable number of the rail sections are not successfully reconstructed, it is still possible to smoothly connect the fitted rail pieces to retrieve a model that if not always accurate for measurements can at least be useful for visualization purposes. Extra challenges in only one side scanned rails have still to be addressed.

In conclusion the answers to the research questions were:

- Can laser range data be effectively used to extract 3D vector models of train rails?

A method demonstrating how point cloud data can be used to produce a 3D vector model of the train rails have been exposed along the document.

- What are the requirements of the data in order to make possible the modelling?

Factors of the dataset as the number of observations in the different faces of the rail or the distribution of the points have been analyzed (read section 4.3.2). Even if the rails present in the available dataset are straight, the methodology has been designed having in mind curved rails all the time, so it is feasible to think a test on such an environment can be as successful as the results here presented.

- What is the internal accuracy of the gauge measurement from the reconstructed rail model?

Although an algorithm on how to measure the track gauge have not been detailed, the followed methodology, fitting individual rails instead of whole track models, allows the possibility of reconstructing both rails in the track and then measure the separation between their internal faces. Nevertheless, such a method will have to face challenges on improving the modelling of only one side scanned rails.

- Is it possible to detect misclassified points during the modelling process?

A method has been described to automatically detect outliers in the rail head. The limitations of this method, as well as the consequences of not handling these misclassification errors have been discussed in section 4.3.3.

- How the different faces of the rail geometry can be identified in the point cloud?

Two automatic methods have been tested as an alternative to manual identification: distance to nearest plane and filtering correspondence. The distance method was highly sensitive to initial values of model parameters making it not suitable for the application as they cannot be pre estimated with the required accuracy. In contrast, filtering showed to be more suitable as it do not require estimating the initial location of the model with respect to the point cloud, but on the other hand it was sensible to outliers in the point cloud. The developed filtering method can be useful to model other objects automatically when it is not possible to accurately estimate the initial location of the model.

- What algorithm can be used to model the curvature of rail objects?

A non-rational Bezier curve algorithm has been explored to smoothly connect all the fitted rail pieces. Regretfully, it has been not compared with other possible algorithms to adjust a curved feature as the rails,

and will have to wait for datasets including curved rails in order to test the proposed method in those circumstances.

- What are the parameters that allow fitting the primitives that compose a rail model?

A set of 7 intrinsic parameters, 2 wear parameters and 6 extrinsic have been identified in order to characterize a rail section.

5.2. Pros and cons of the method

5.2.1. Advantages

As a method to obtain the model of a rail is still a novelty, most of the characteristics of the methodology cannot be compared and must be considered an improvement even if they are not successful under all circumstances.

One of the main advantages is the method is fully automatic, requiring only the input of the dataset and deciding the piece length and the correspondence algorithm.

As for the final modelling of the rail curvature using Bezier curves, it is able to fill gaps from the dataset or from failure to fit some of the rail pieces during the fitting step. Additionally, it smoothly adjusts to orientation, rotation and slope of the rail, being able to calculate all the extrinsic parameters of a rail profile in any point of the rail.

In order to fit the model to the point cloud, having points in the head of the rail is enough to reconstruct the object. The full geometry of the rail is reconstructed maintaining the distance and angular constraints of the different faces of the object, in opposition to what can be obtained by a general purpose mesh adjustment.

As the rail is modelled individually, instead of constraining the relation of the two rails of each track, it is possible to measure the gauge between two rail models to detect problematic areas, and to adapt the method to three rails tracks.

With respect to the acquisition system, the process is only dependant on single echo laser data, not requiring frequency, full-waveform or other lidar information. Indeed, the use of laser scanning as the acquisition tool, make the method independent of the light conditions, making the overall method suitable for use at night during train valley hours. In fact, mobile laser scanning is improving its accuracy every year and it is possible that higher density and better accuracy point clouds may be available in the future years opening new opportunities for the methodology.

The method is deterministic; this is, if run over the same dataset with the same initial parameters the resulting model is always the same, making the different tests varying some parameters as the piece length easily comparable.

With respect to the implementation, the method has been fully implemented in python using object-oriented programming, enabling extension and substitution of algorithms at any step of the process. It also ensures it is possible to smoothly run the algorithm from an input dataset to a resulting model without having to manually link intermediate steps, although it is possible to do it if desired thanks to python scripting interactivity abilities. Additionally, the output result follows the open standard COLLADA, which ensures the compatibility with the most popular 3D modelling software.

5.2.2. Disadvantages

One of the main problems is the filtering correspondence method is not robust to outliers and they must be detected to limit their impact. Additionally it is also sensible to the orientation of the rail, although it is

possible to avoid this problem by previously estimating the orientation of the rail axis, process that will also improve the sectioning method. In a similar way the filtering and fitting steps are affected by the presence of certain elements in the head of the rail, as guard rails or joint bars.

One of the drawbacks of using mobile laser scanning devices is only the internal faces of the rail track are usually scanned. In more than one track railways it is possible to scan both sides of the central rails combining the different acquisition strips, which may lower the precision of the dataset depending on the quality of their registration. Even still, the lateral rails are scanned only in one side. Nevertheless, the modelling method is independent of the acquisition process, and it is directly applicable to other lidar sources as long as they can retrieve the rail of the head with enough point density.

Being the detection of outliers so important for the correspondence filtering step, the method for that purpose implemented in this study relies in principal component analysis, which is not applicable in only one side scanned rails. It is necessary to develop a different outlier detection algorithm able to work when only one lateral of the rail has been scanned.

With respect to the intrinsic parameters of the rail, they are treated as input information depending on the rail type, and thus require pre-knowledge of the track to be modelled. Nevertheless, it is possible to pre-process the rail to assess which rail model is being used in each section, being the number of possible types quite limited, and generally constant along the same railway track.

The model is limited to assessing the extrinsic parameters that define the rail, its location and curvature, but has not addressed how to assess the wear of the rail. If the acquisition method was able to acquire both laterals of the rail, the method could be easily extended to model the horizontal wear. As for the vertical wear, the limitation is the outliers in the foot, which are produced by the presence of other track elements, as the bolts or the ballast. In case these elements could be detected or just filtered out, the correspondence method can be extended to retrieve also the foot faces, opening the opportunity to model the vertical wear of the rail. However, it is possible that the wear is not observable if it is too small in comparison with the accuracy of the acquisition method.

The methodology requires that the points belonging to the rail are detected in a pre-step and used as input. Additionally, each rail in the track should be individually identified in order to model the rails one by one. This precondition has been fulfilled by a parallel project in ITC, but this method will require manual identification in the cases where that automatic algorithm is not applicable.

The surface of the rail is approximated in the final model using triangular planes, which do not adjust to the real curved surfaces produced by the torsion and other deformations of the rail. The effect of this approximation is magnified when using larger piece lengths, but it can be reduced by increasing the number of Bezier points to produce the curved model, at the cost of increasing the validation time and increasing the output file volume.

The parametric model used in this study is quite simple when compared to real rails design. Even if the result of this approximation may be acceptable as the introduced error is much less to the noise of the dataset, it might be possible to improve the modelling result, or at least the visualization replacing the simple model by a more complex one.

5.3. Open challenges and possible follow-ups

There are still open research lines to improve the understanding and results of rail modelling using laser point clouds. First of all, it is possible to improve the reconstruction of only one side scanned rails, by automatically detecting what side was scanned and profit that knowledge, besides of developing an outlier detection algorithm capable of handling such datasets.

The sectioning and filtering steps can benefit from having better initial estimations of the rail orientation, which can be done using the rail axis that have been successfully reconstructed from lidar point clouds by other studies (Beger et al., 2011), and can be even retrieved from the GPS signal of the mobile laser device when it is available.

One of the main limitations of this research has been the availability of only one dataset to test the method, and the fact that it do not includes curved rails or switches. In order to accept the method as functional, it must be tested against other datasets and especially one including curved rails. It might be possible from such a dataset to test curve models different to the non-rational Bezier used here, in order to test which one adapts better to railway tracks.

Due to the large effect of incorrect piece translation parameters in the final model, it remains open the possibility to automatically check when a piece fitting is feasibly correct or not to improve the final results. Statistical analysis of the changes in the adjusted parameters, and comparing the resulting parameters of one rail to those of the neighbours can be a line to follow in this issue.

Additionally, the horizontal wear of the rail may be assessed by finding the points corresponding to the foot of the rail. Filtering can be extended to those planes if the outliers produced by the presence of bolts, ballast and other objects are removed from the input point cloud.

In order to automatically detect the rail type of certain railway line, it can be interesting to build up a database with the different possible models, so the type present in the point cloud can be detected by checking which one minimizes the distance from the points to the reconstructed model.

With respect to other railway objects, the correspondence filtering method developed in this thesis can be adapted in order to model them using constrained parametric models and surface fitting. As for the wires, it would be possible to use non-rational Bezier curve adjustment to model them but the quality of the result would depend on the distribution of the control points and the relation of the wire width and its curvature.

Finally, adjustment of curved models seems a promising alternative to the straight pieces fitting to reconstruct curved rails, and it has been already applied to similar objects as curved kerbstones (Liang & Vosselman, 2012). Although it will require a complete different approach, it still can profit the knowledge of rail modelling characteristics highlighted by this research.

LIST OF REFERENCES

Alippi, C., Casagrande, E., Fumagalli, M., Scotti, F., Piuri, V., & Valsecchi, L. (2002). An embedded system methodology for real-time analysis of railways track profile. *IMTC 2002: Proceedings of the 19th IEEE Instrumentation and measurement*, 747-751.

Anton, H. (1994). *Elementary linear algebra* (7th ed.). United States: Wiley & Sons.

Arastounia, M. (2012). *Automatic classification of lidar point clouds in a railway environment.* To be published master's thesis. ITC University of Twente.

Beger, R., Gedrange, C., Hecht, R., & Neubert, M. (2011). Data fusion of extremely high resolution aerial imagery and LiDAR data for automated railroad centre line reconstruction. *ISPRS Journal of Photogrammetry and Remote Sensing, 66*(6, Supplement), S40-S51.

Campbell, N. (2012). Lecture notes on Computer Graphics. University of Bristol.

Evans, J., & Berg, M. (2009). Challenges in simulation of rail vehicle dynamics. *Vehicle System Dynamics, 47*(8), 1023-1048.

Federal Railroad Administration Office of Safety Analysis. (2011). Railway accident causes. Retrieved May 28, 2011, from http://safetydata.fra.dot.gov/OfficeofSafety/publicsite/Query/inccaus.aspx

Grassie, S. L. (1996). Measurement of railhead longitudinal profiles. A comparison of different techniques. *Wear, 191*(1-2), 245-251.

Guler, H., Jovanovic, S., & Evren, G. (2011). Modelling railway track geometry deterioration. *Proceedings of the Institution of Civil Engineers-Transport, 164*(2), 65-75.

Jaakkola, A., Hyyppa, J., Hyyppa, H., & Kukko, A. (2008). Retrieval algorithms for road surface modelling using laser-based mobile mapping. *Sensors, 8*(9), 5238-5249.

Jwa, Y., & Sohn, G. (2010). Extraction of railroad objects from very high resolution helicopter-born lidar and ortho-image data. *International Archives of Photogrammetry, Remote Sensing and Spatial Information Sciences, 38*(3A), 97-102.

Li, D., Meddah, A., Hass, K., & Kalay, S. (2006). Relating track geometry to vehicle performance using neural network approach. *Proceedings of the Institution of Mechanical Engineers, Part F: Journal of Rail and Rapid Transit, 220*(3), 273-281.

Liang, Z., & Vosselman, G. (2012). Mapping curbstones in airborne and mobile laser scanning data. *Journal of Applied Earth Observation and Geosciences.* To be published.

Marino, F., Distante, A., Mazzeo, P., & Stella, E. (2007). A real-time visual inspection system for railway maintenance: Automatic hexagonal-headed bolts detection. *IEEE Transactions on Systems Man and Cybernetics Part C-Applications, 37*(3), 418-428.

Mazzeo, P. (2004). Visual recognition of fastening bolts for railroad maintenance. *Pattern Recognition Letters, 25*(6), 669-677.

Neubert, M., Hecht, R., Gedrange, C., Trommler, M., Herold, H., Krüger, T., & Brimmer, F. (2008). Extraction of railroad objects from very high resolution helicopter-born lidar and ortho-image data. *International Archives of Photogrammetry, Remote Sensing and Spatial Information Sciences, 38*(4/C1), 25-30.

Papaelias, M., Roberts, C., & Davis, C. (2008). A review on non-destructive evaluation of rails: state-of-the-art and future development. *Proceedings of the Institution of Mechanical Engineers, Part F: Journal of Rail and Rapid Transit*, *222*(4), 367-384.

Rabbani Shah, Tahir. (2006). *Automatic reconstruction of industrial installations: using point clouds and images*. Doctoral dissertation. Nederlandse Commissie voor Geodesie (NCG), Delft.

Sadeghi, J., & Askarinejad, H. (2010). Development of improved railway track degradation models. *Structure and infrastructure engineering*, *6*(6), 675-688.

Sande, C. van der, Soudarissanane, S., & Khoshelham, K. (2010). Assessment of Relative Accuracy of AHN-2 Laser Scanning Data Using Planar Features. *Sensors*, *10*(9), 8198-8214.

Smith, L. (2002). A Tutorial on Principal Component Analysis. Retrieved December 16, 2011, from http://www.cs.otago.ac.nz/cosc453/student_tutorials/principal_components.pdf

Vosselman, G., & Maas, H.-G. (2010). *Airborne and terrestrial laser scanning*. United States: Whittles Publishing.

Weston, P., Ling, C., Goodman, C., Roberts, C., Li, P., & Goodall, R. (2007). Monitoring lateral track irregularity from in-service railway vehicles. *Proceedings of the Institution of Mechanical Engineers, Part F: Journal of Rail and Rapid Transit*, *221*(1), 89-100.